Chapter 4
Mechanical Properties of the Body

Abstract The composition and structure of the structural components of the body, including bones, ligaments, tendons, and cartilage, are first presented. The mechanical properties of these body components begin by investigating their stress-strain relationships in the harmonic regime. Analysis is improved by modeling their nonlinear, time-dependent properties and then their time-dependent, viscoelastic properties. These models are used to understand how bones can bend under unusual conditions, and the occurrence of fractures and sports injuries, along with ways to avoid these unwanted events.

We now examine the mechanical properties of organs and components of the body. In subsequent chapters we will consider their other materials properties, specifically their thermal, electrical, and optical properties. We need to understand these mechanical properties to evaluate how body components function and to assess the impact of injuries. They are also essential in assessing the suitability of biomedical devices, such as hip replacements. Research and development teams are rightly concerned with how human bodies react to such prosthetic devices in a biochemical sense and whether they will "reject" the implants. They are equally concerned with how such implants match the other body components in a mechanical sense [8] (Problems 4.13 and 4.14, Fig. 4.79). For example, if they are softer than what they replace, they will wear out; if they are harder, there could be excessive wear on other body parts. In Chap. 3 we also saw how human motion is affected by the mechanical properties of objects outside the body, such as running shoes, floors, and vaulting poles.

Our goal in this chapter is to characterize the mechanical behavior of body components by using basic models that are routinely used in materials science and engineering. Once we have modeled the body component, we will use that model to understand the consequences of that modeled property, such as: For a given impact, will the bone break or just bend?

These mechanical properties all have a biological basis that is very complex and this will not be discussed here. Much of these details are still not understood well

I.P. Herman, *Physics of the Human Body*, Biological and Medical Physics, Biomedical Engineering, DOI 10.1007/978-3-319-23932-3_4

at all. We will assume that these properties have known averages among humans. There are distributions about these averages due to variations in our genes, gender, age, health, past injuries, and so on.

From a mechanical perspective, the different parts of the body can be classified in a variety of ways. For example, components can be either *passive* or *active*. Passive components, such as bones and tendons, respond to outside forces. Active elements, muscles, generate forces. This division is not perfect. Muscles are indeed active elements, but they also have some properties of passive components, and when they are modeled, the model must include both their active and passive properties. These passive elements and properties are discussed in this chapter. Active elements are discussed in Chap. 5.

The response of passive elements to applied stresses (forces/area) is by no means simple. Passive components can respond to forces in ways that are either independent or dependent of time. By this we mean that the component can respond to only currently applied forces or to both current forces and forces applied earlier.

The simplest type of passive response is *harmonic or Hookean* behavior, in which the properties of the material behave exactly like that of an ideal harmonic oscillator spring. Deformations are linear with the applied forces and stresses. The response is independent of time. All the potential energy stored in such media can be extracted. Bones and tendons are fairly well (but not perfectly) modeled as such elastic media. The elastic nature of tendons makes them very important in energy storage and retrieval during motion. Some materials systems, such as metal springs and bones, behave similarly under *tension* and *compression*. Others, such as cartilage and tendons, do not. (Why?)

No material is perfectly harmonic. Most materials deviate from perfectly harmonic behavior for large applied forces and large deformations. A material can deviate from a harmonic oscillator dependence with the deformation depending nonlinearly on force or stress, and yet this deformation can still be reversible. This means that the material returns to its initial state when the stress is removed both in the linear and nonlinear parts of this *elastic regime or region* (see Fig. 4.1). For even larger stresses, the material is no longer elastic because it undergoes *plastic deformation*, which is irreversible. This means that the material never returns to the same size or shape when the stress is removed. For even larger stresses, there is *fracture*. One glaring example is the fracture of bones.

Whereas elastic behavior is independent of history and enables total recovery of stored energy, this is not so in the opposite extreme of *viscous* behavior, for which the response depends on the history of applied stresses and no energy is recoverable. Viscous materials dissipate energy; friction is one manifestation of viscous behavior. Most materials have properties that are in part elastic and in part viscous, and as such are *viscoelastic*. We will examine models describing such viscoelasticity.

We will need to distinguish between the *intensive* and *extensive* properties of the body component (or any other object). Let us say we were to examine a $100\,\text{cm}^3$ ball of solid iron that has a 787 g mass. Obviously, the iron ball has a mass density of $787\,\text{g}/100\,\text{cm}^3 = 7.87\,\text{g/cm}^3$. This property per unit volume is an *intensive* property.

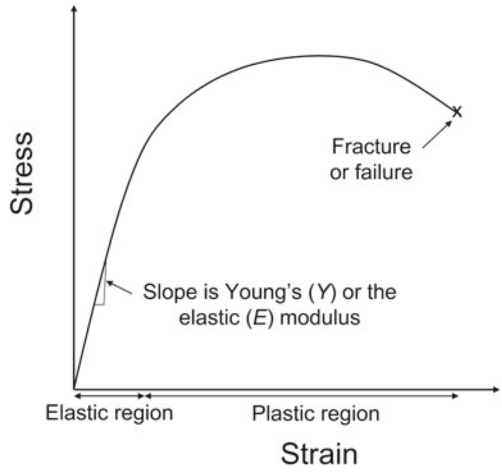

Fig. 4.1 General stress—strain relationship. For more detail, see Fig. 4.15

It does not depend on the size or shape of the ball and applies to any object composed of this type of iron. An *extensive* property of this ball is that it has a mass of 787 g; another is its 100 cm^3 volume. Such extensive properties depend on the intensive property of the object and the size and shape of the object.

Why do some people's bones break more readily than others? There are several reasons: (a) They could have different intensive properties. For example, they could be more porous and concomitantly have lower damage thresholds—such as for those with *osteoporosis*, which is common in older people who have lost much calcium. (b) They could have different extensive properties, such as thinner bones. Part of this is clearly genetic in origin, but some is developmental. Bones become thicker in children who are physically active, and who are consequently applying loads to them while they are growing [30, 41, 42]. In fact, the bones in the arm wielding the tennis racket can be ~30% thicker than those in the other arm in adults who played tennis as youngsters [35]. (c) They could have bad luck. Reason (a) is related to why body materials are complex. They are *composite* materials, composed of different types of materials on a microscopic basis, that depend on life experiences. Bone is a composite composed of calcium-based inorganic matter and organic matter.

We have already seen the implications of several of these mechanical properties. In analyzing running in Chap. 3 we saw that about a third of the kinetic energy lost each time the foot hits the ground goes into stretching the Achilles tendon, and that most of this energy is recoverable (which is consistent with nearly elastic behavior). In modeling throwing a ball, we neglected any friction about the elbow joint during the throwing motion. This followed our discussion of the very low coefficient of friction in synovial joints. In our discussion of collisions, we saw that the tibia can break if we jump stiff-legged from a height of only 1 m (which is fracture). Our model of throwing a ball used the force generated by the biceps brachii (which is an active element).

Interesting references for these materials properties include [6, 8, 9, 22, 27, 31, 45, 47, 56, 57, 59, 61]. Reference [64] examines quite extensively the materials of the body and materials used in medicine. Mechanical properties are given in [1, 17, 79].

4.1 Material Components of the Body

We will briefly characterize some of the major structural components of the body: bones, and several soft materials, such as ligaments, tendons, and cartilage, and then analyze their mechanical properties. More generally, there are four categories of tissues:

(1) *Epithelial tissue* covers the body and lines organs or secretes hormones. It has closely packed cells, little intercellular material, nerves, and no blood vessels (and so it is *avascular*).

(2) *Connective tissue* includes bone, cartilage, dense connective tissue (such as ligaments and tendons), loose connective tissue—such as "fat"—and blood and lymph vascular tissue. Most connective tissue has nerves and scattered cells in a background called a matrix. There are many blood vessels in bone and at the periphery of the menisci—and so they are highly *vascularized*, but tendons, ligaments, and (the bulk of) cartilage are not. The matrix consists of fibers and ground substances. The fibers include collagen fibers (made of the protein *collagen*) that are tough and flexible; elastic fibers (made of the protein *elastin*) that are strong and stretchable; and reticular, web-like fibers. The ground substance includes cell adhesion proteins to hold the tissue together and proteoglycans to provide firmness.

Epithelial membranes consist of epithelial and connective tissue. These line the body (skin (*cutaneous* membrane)), internal organs (*serous* membranes of the heart (*pericardium*), lungs (*pleura*), and abdominal structures (*peritoneum*)), cavities that open to the outside world (*mucous* membranes of the nasal cavity, and the respiratory, gastrointestinal, and urogenital tracts), and cavities at bone joints (*synovial* membranes).

(3) *Nervous tissue*, for body control, consists of *neurons* to transmit electrical signals and neuroglia (or glial cells) to support the neurons, by insulating them or anchoring them to blood vessels.

(4) *Muscle tissue* controls movement, and includes passive components (such as in the connective tissue) and active, motor-like components. Its structure and properties will be detailed in Chap. 5.

The different fractions of the common building blocks in these components are shown in Fig. 4.2.

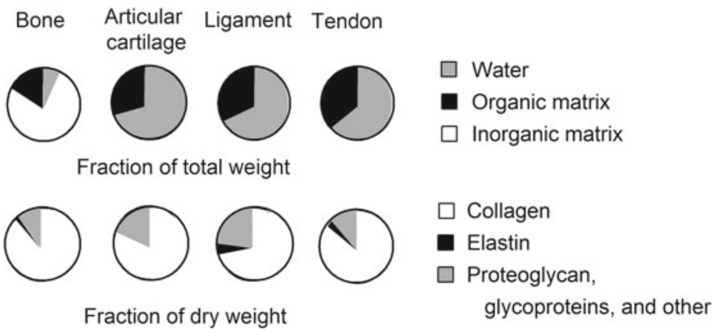

Fig. 4.2 Typical composition of several human musculoskeletal structural components by fractional total and dry weight. (Based on [4])

4.1.1 Bone

Bones provide a structural framework to attach muscles and organs, enable movement through the attachment of muscles, provide physical protection of organs (such as the skull for the brain and the rib cage for the lungs), store minerals (calcium and phosphorus) and some fats (in the yellow marrow), and produce red blood cells (in the red marrow). The stiff nature of bone clearly enables it to form a semirigid framework, enable motion (because how could muscles do their job with flexible bones?), and provide organ protection. We will see it also means that large bones can serve these functions and still be hollow and filled with the soft marrow. There are long bones, as in the arms and legs; short cube-like bones; flat bones, as in the skull and ribs; and irregularly shaped bones, as in the pelvis and vertebrae.

Bone is a complex composite material, with living and nonliving matter. The living matter includes the cells osteoblasts and osteoclasts, which, respectively, make new bone and resorb (erode) existing bone, and osteocytes, which are former osteoblasts buried in bone they have made. Bone experiences net growth during childhood (with osteoblasts outperforming osteoclasts), steady state during most of adulthood (with the effects of osteoblasts and osteoclasts balancing each other), and net decrease in older age (with osteoclasts outperforming osteoblasts), leading to osteoporosis [71]. Excluding water, the nonliving matter of bone is 40% by weight (60% by volume) collagen and 60% by weight (40% by volume) calcium hydroxyappatite ($Ca_{10}(PO_4)_6(OH)_2$). The $\sim$5 nm $\times$ 5 nm $\times$ 40 nm rod or plate crystals with hexagonal symmetry of the ceramic-like calcium hydroxyappatite are bound by the elastomer-like collagen. The inorganic ceramic component gives compact bone its large strength (a large elastic constant Y) and a large ultimate compressive stress (UCS). The collagen component makes bone much more flexible than a ceramic and much more stable under tension and bending. If you let a turkey leg sit for 24 h in 1 M HCl it becomes very flexible because the ceramic crystals have been dissolved and all that remains is a collagen structure [10]. About 1% of the organic component is proteoglycans (mucopolysaccharides). About 25% of the volume of bone is water, $\sim$60% of which is bound to the collagen. Spongy (or trabecular) bone has voids with lateral dimensions of 50–500 μm.

Figure 4.3a shows the structure of a typical long bone, such as the femur. It has a long tubular shaft, the *diaphysis* (die-a'-phi-sus), which is a relatively thin shell of *compact, cortical, or dense bone* for strength. We will see later in this chapter that this type of hollow design maintains much of the strength of the corresponding solid structure, but with much less weight. At either end, the shaft broadens to form the *epiphyses* (e-pi-fi-sees'), where there is an overlayer of articular cartilage for lubrication and inside the bone, beneath the compact bone, is *trabecular, cancellous, or spongy bone*, which is a porous mesh of trabeculae (tra-bic'-you-lee) that can absorb shock. This porous bone is also found in the bones in the spinal column, where it provides some structural support and absorbs shock. Figure 4.3b shows

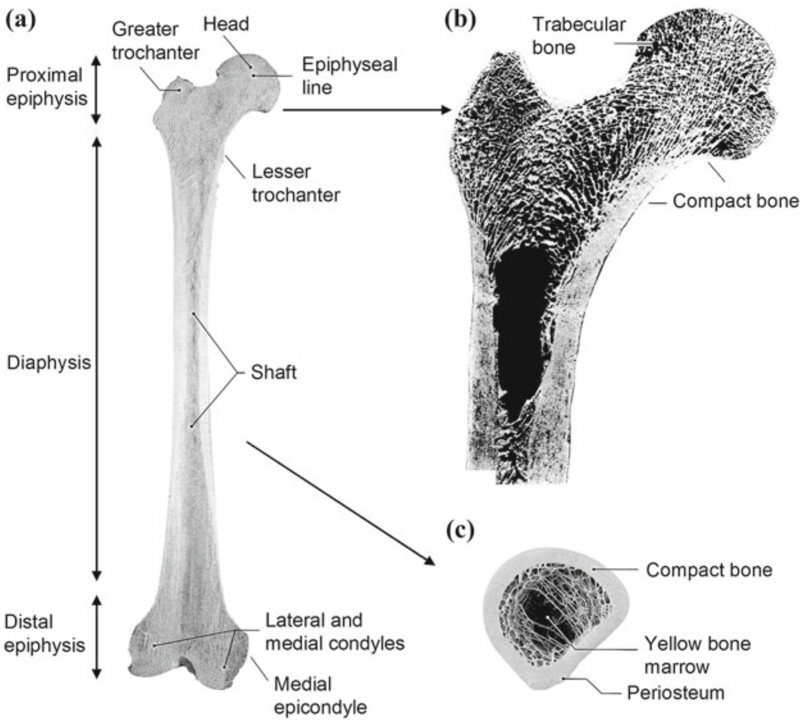

Fig. 4.3 Structure of a long bone, as exemplified by the femur, with a **a** schematic of the frontal section, **b** photo of the proximal epiphysis, and **c** schematic of the cross-section of the diaphysis. (**b**) is a photograph of a coronal section of the upper end of the femur of a 31-year-old male. The cut passes through the head, neck, greater trochanter, and part of the shaft, and is off-center between the middle and posterior thirds. The uniform sections are compact bone, while the meshed regions are trabecular bone. (From [75] (for (**a**), (**c**)) and [77] (for (**b**)))

that the layer of cortical bone in the shaft is thick and it becomes relatively very thin at the proximal end, where it surrounds the trabecular bone. There is bone marrow in the hollow shaft, the diaphysis. In short and irregular bones, spongy bone is encircled by a thin layer of compact bone, while in flat bones it is sandwiched by it.

4.1.2 Ligaments and Tendons

Ligaments and tendons are dense connective tissue with a dense network of fibers, with few cells and little ground substance. Ligaments are tough bands of fibrous connective tissue. They are 55–65% water and 35–45% dry matter, which consists of 70–80% collagen (mostly type I), 10–15% elastin, and a small amount, 1–3%, of proteoglycans. The collagen (Fig. 4.4) gives ligaments their high tensile strength. The collagen helices assemble into microfibrils (4 nm in diameter), which assemble into subfrils (20 nm in diameter), which assemble into fibrils (50–500 nm in diameter), and then into collagen fibers (100–300 μm in diameter) with fibroblast cells that synthesize the collagen.

The dry weight of tendons is 75–85% collagen (95% type I and 5% type III or V), <3% elastin, and 1–2% proteoglycans. The structural hierarchy (Fig. 4.5) is like that of ligaments except they are arranged into packets called fascicles. Also, the bundles of collagen fibers are more parallel in tendons than in ligaments, as seen in Fig. 4.6.

In contrast, the dry matter of skin is 56–70% collagen (mostly type I), 5–10% elastin, and 2–4% proteoglycans.

In each of these soft materials, the collagen gives it tensile strength, while the elastin gives it elasticity, which is more important in ligaments than in tendons.

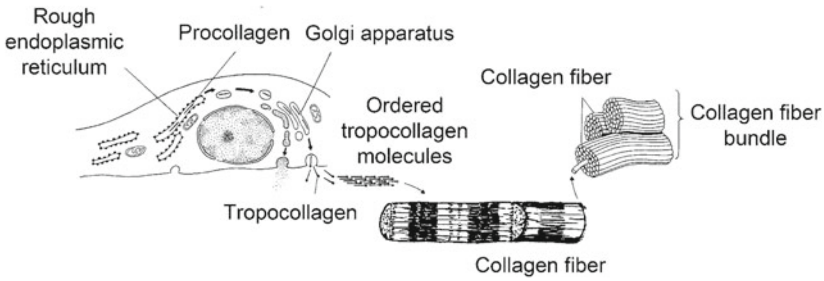

Fig. 4.4 Structure of collagen in fibers and bundles in tendons and ligaments, with ordered arrangement of collagen molecules in the microstructure. See Fig. 4.5 for more details about structure. (From [72])

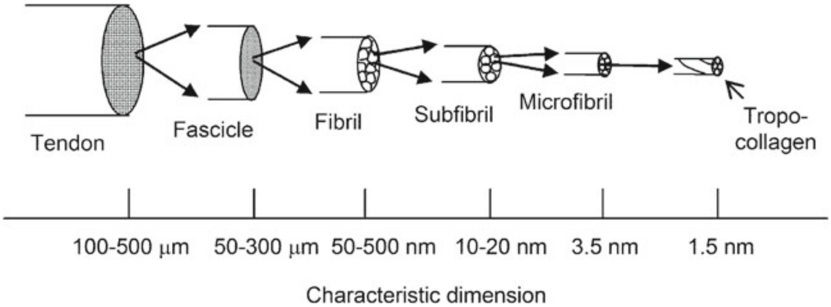

Fig. 4.5 Hierarchical structure of tendons. (Based on [4, 37])

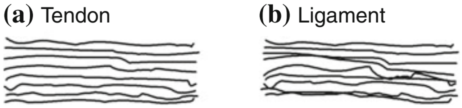

Fig. 4.6 Collagen fibers are (**a**) parallel in a tendon and (**b**) nearly parallel in a ligament. (Based on [58])

4.1.3 Cartilage

There are three types of cartilage: *Hyaline* (high'-uh-lun) *cartilage*, the most common in adults, is found in the ventral ends of ribs and covering the joint surfaces of bones. *Elastic cartilage* is more flexible, and is found in the external ear and eustachian tubes. *Fibrocartilage* occurs in the intervertebral disks. Cartilage that lines the bones in synovial joints (1–6 mm thick) is also called *articular cartilage*; it serves as a self-renewing, well-lubricated load bearing surface with wear prevention. It is most often hyaline cartilage, except in joints, such as the knee (the menisci), which contain fibrocartilaginous disks.

Articular cartilage is not meant to serve as a shock absorber to cushion forces or slow joint rotation [45], because it is so thin that it can absorb very little energy even though it is less stiff than cortical bone. In fact, it absorbs much less energy than muscles resisting joint rotation (eccentric contractions, Chap. 5) or the bones on either side of the joint (see Problem 4.12). About 30% of cartilage by mass is a solid matrix of collagen (40–70% of the dry mass, ∼80% type II collagen and several other types: V, VI, IX, X, and XI) and proteoglycan (15–40% of the dry mass) and 70% is water and inorganic salts (as seen the structure in Fig. 4.7). Chondrocyte cells that manufacture the cartilage organic material comprise less than 5–10% of the volume. Cartilage is viscoelastic because it is a very flexible, porous material (50 Å voids) with voids that are filled with water. The water dissipates energy as it flows through the voids under compression.

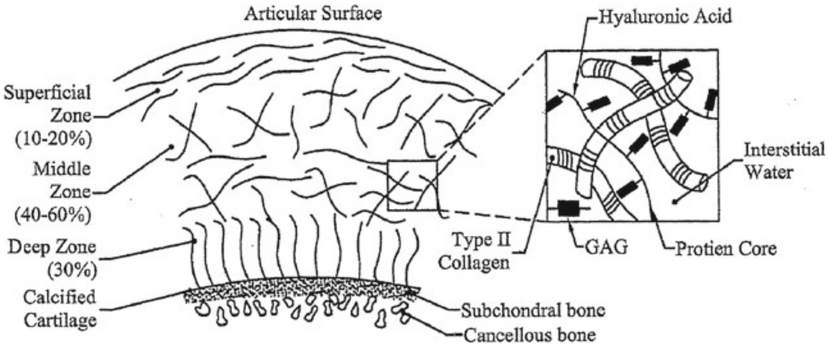

Fig. 4.7 Structure of articular cartilage, showing its inhomogeneity and solid—fluid constitution. The inset shows the local molecular organization of cartilage. (From [34])

In tension the collagen of the solid phase carries most of the load, while in compression both the solid and liquid phases carry the load. The viscoelasticity of cartilage is controlled by the exudation of the fluid through the pores in this biphasic material that is responsible for the lubrication of synovial joints.

4.2 Elastic Properties

4.2.1 Basic Stress–Strain Relationships

In the harmonic regime, elastic materials are modeled as perfect springs obeying Hooke's Law. This is usually expressed as

$$F = -kx, \tag{4.1}$$

where F is the force felt by an object attached to a spring, with spring constant k, when the spring is extended a distance x. When the spring is extended a distance x, say to the right, the attached body feels a restoring force kx to the left (Fig. 4.8).

In examining such Hookean materials we will need to alter this viewpoint a bit. There is a length of spring or material for which there is no restoring force. We will call this equilibrium length x_0. In (4.1), x is implicitly the deviation from this equilibrium length, the *deformation*. For reasons that will become clear soon, we prefer to refer x to this equilibrium length and so

$$F = -k(x - x_0). \tag{4.2}$$

Also, in studying problems with springs, we usually examine the effect of the spring forces on other masses. Here we are concerned with the effect of other forces

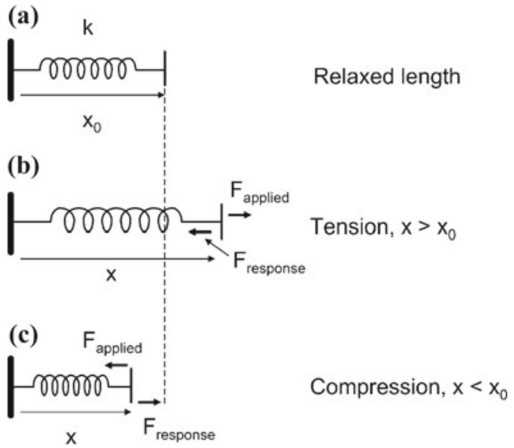

Fig. 4.8 Spring model of elastic materials, **a** relaxed, **b** under tension, **c** under compression. The text calls the material length L instead of x

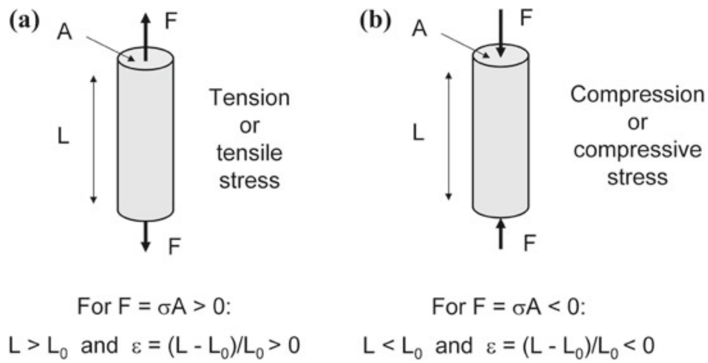

Fig. 4.9 Cylinder of relaxed length L_0 **a** under tension and **b** under compression

on materials modeled as springs. Therefore we consider the force applied to the spring-like object, F_{applied}, which is the negative of the above force F felt by the object attached to the spring, and is

$$F_{\text{applied}} = k(x - x_0) = k(L - L_0). \tag{4.3}$$

We have also changed notation so that length of the material is L and its relaxed length is L_0.

When $L = L_0$ the material is relaxed. When there is a positive F_{applied} (Figs. 4.8b and 4.9a), the material is under *tension* and $L > L_0$. When there is a negative F_{applied} (Figs. 4.8c and 4.9b), the material is under *compression* and $L < L_0$.

Equation (4.3) represents the extensive properties of the material. While this is very important, we first want to examine the intensive properties of the material. If the object has a cross-sectional area A and length L, we can rewrite (4.3) as

$$\frac{F_{\text{applied}}}{A} = \frac{kL_0}{A}\frac{L - L_0}{L_0}. \tag{4.4}$$

Each fraction represents an intensive parameter. The applied force/area, F_{applied}/A, is called the stress σ. The fractional increase in length, $(L - L_0)/L_0$, is called the strain (or the engineering strain) ϵ. $L - L_0$ is the elongation. The normalized spring constant, kL_0/A, is called either Young's modulus or the elastic modulus and is represented by Y (or E). This modulus is a fundamental intensive property of the material. Consequently,

$$\sigma = Y\epsilon. \tag{4.5}$$

This linear *constitutive* relationship describing this material is valid only for small strains. It is usually valid for $|\epsilon| \ll 1$, but the range of validity really depends on the type of material. We have ignored any change in cross-sectional area. There is usually a change in A with a change in L (see below), which we will usually ignore here.

As seen in Fig. 4.8, tensile stress means $\sigma > 0$ and leads to a tensile strain $\epsilon > 0$. A compressive stress means $\sigma < 0$ and leads to a compressive strain $\epsilon < 0$. For such elastic materials in the *proportional (or harmonic or Hookean) regime* the stress–strain relation is linear, as is seen in Fig. 4.1. The units of stress σ and modulus Y are both those of force/area, such as N/m^2 (= 1 Pa) or the more convenient unit of N/mm^2 (= 1 MPa); we will usually use these last two equivalent units. Strain, ϵ, is unitless. Remember from Table 2.6 that $1\,\text{N/mm}^2 = 10^6\,\text{N/m}^2 = 1\,\text{MPa} = 145\,\text{psi}$.

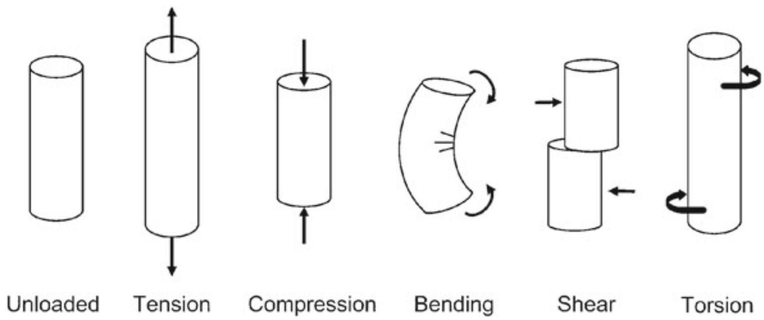

Fig. 4.10 Schematic of various loading modes. (Based on [58])

4.2.2 Other Stress–Strain Relations

In addition to these linear relations between stress and strain, there are other types of deformations (Fig. 4.10). Figure 4.11a shows the geometry of shear deformations with force F and shear stress $\tau = F/A$. (τ is not torque here.) The response is the shear strain $\gamma = \tan\theta$, and for small deviations $\gamma \approx \theta$. The shear stress and strain are related by

$$\tau = G\gamma, \tag{4.6}$$

where G is the shear modulus. This shear deformation is related to the torsion of the top of a cylinder, with the bottom fixed, as seen in Fig. 4.11b, where the torsion T is related to the deformation angle ϕ.

Let us consider the deformation of a cylinder with the long axis along the z-axis. We have already called the *axial strain* response in the z direction ϵ, but because stresses lead to strain deformations in different directions, we could be more specific (for the moment) and call it ϵ_z. We assumed earlier that the cross-sectional area of such a cylinder does not change under tension or compression, but it does to a certain extent. We will call the fractional strains in these lateral x and y directions—the *lateral or transverse strains*—ϵ_x and ϵ_y, respectively. (In more advanced discussions, these three x , y, and z components of strain are really referred to as ϵ_{xx} , ϵ_{yy}, and ϵ_{zz}.) For the linear deformation described above, symmetry implies that $\epsilon_x = \epsilon_y$. For a given material there is a relationship between these longitudinal and lateral strains provided by Poisson's ratio

$$\upsilon = -\frac{\epsilon_x}{\epsilon_z}. \tag{4.7}$$

For isotropic materials, the range of possible υ is $-1 < \upsilon < 0.5$, although materials with negative υ are not found in nature. For anisotropic materials, such as many materials in the body, υ can exceed 0.5. For metals and many engineering materials $\upsilon = 0.25 - 0.35$, but it tends to be higher for biological materials. For bone, υ ranges from 0.21 to 0.62 [47]. For tissues like those in the brain, $\upsilon \sim 0.5$.

After this deformation the new volume is the old one $\times$ $(1+\epsilon_x)(1+\epsilon_y)(1+\epsilon_z) \approx 1 + \epsilon_x + \epsilon_y + \epsilon_z$, when each strain has magnitude $\ll 1$ (Fig. 4.12). Using Poisson's ratio, the new volume is $1+(1-2\upsilon)\epsilon_z$ $\times$ the old volume and the fractional change in the volume is $\epsilon_x + \epsilon_y + \epsilon_z = (1-2\upsilon)\epsilon_z$. For example, with $\upsilon = 0.25$ this fractional

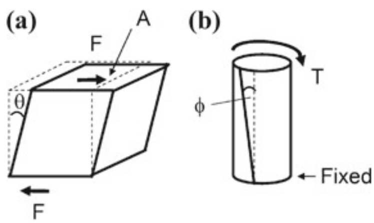

Fig. 4.11 Shear and torsion forces. **a** Shear. **b** Torsion

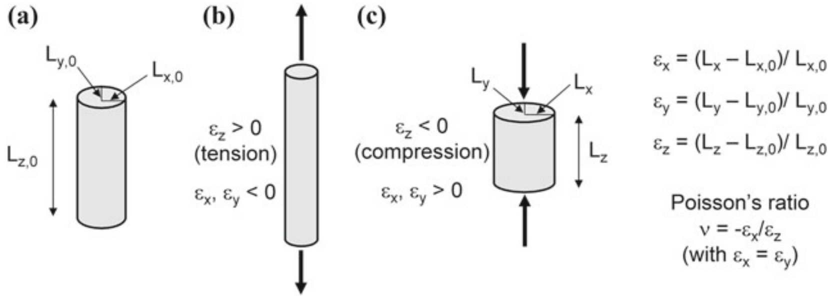

Fig. 4.12 Changes in lateral dimensions during (**b**) tension and (**c**) compression, as determined by Poisson's ratio, compared to those with no forces applied in (**a**)

volume change is $0.5\epsilon_z$. If $\upsilon = 0.5$, there is no volume change even with the change in shape. Similarly, after deformation the new cross-sectional area is the old one $\times\ (1+\epsilon_x)(1+\epsilon_y) \approx 1+\epsilon_x+\epsilon_y = 1-2\upsilon\epsilon_z$, and the fractional change in area is $\epsilon_x+\epsilon_y = -2\upsilon\epsilon_z$.

Like Y and G, υ is an intensive property of the material. For isotropic materials they are interrelated by

$$Y = 2G(1+\upsilon). \tag{4.8}$$

For example, if $\upsilon = 0.25$, the shear and elastic moduli are related by $G = 0.4Y$.

4.2.3 *Bone Shortening*

How much do our bones shorten under compression? We will assume that the relation $\sigma = Y\epsilon$ is valid until the stress reaches its maximum just before fracture occurs, which is called the *ultimate compressive stress* (UCS) and which is 170 MPa for compact bone; this is a good approximation for this calculation. Then $\sigma = Y(L-L_0)/L_0$ and the bone shortens by

$$\Delta L = L - L_0 = \frac{\sigma L_0}{Y} \tag{4.9}$$

and fractionally by

$$\epsilon = \frac{\Delta L}{L_0} = \frac{\sigma}{Y}. \tag{4.10}$$

How much does the femur shorten when you stand on one foot? With no stress the femur is $L_0 = 0.5\,\text{m} = 500\,\text{mm}$ long. The body weight of 700 N

(70 kg) is distributed over the femur cross-sectional area A $= 370\,\mathrm{mm}^2$, so $\sigma = 700\,\mathrm{N}/370\,\mathrm{mm}^2 = 2.1\,\mathrm{N/mm}^2 = 2.1\,\mathrm{MPa}$. The femur shortens by only $\Delta L = (\sigma/Y)L_0 = ((2.1\,\mathrm{N/mm}^2)/(179 \times 10^2\,\mathrm{N/mm}^2))\,500\,\mathrm{mm} = 0.06\,\mathrm{mm}$. This corresponds to a strain of $\Delta L/L_0 = \sigma/Y = (2.1\,\mathrm{N/mm}^2)/(179\times 10^2\,\mathrm{N/mm}^2) = 0.01\%$. In units of microstrain (10^{-6} mm/mm), this is 100 microstrain (or 100 $\mu\epsilon$).

The maximum stress in compression is the UCS. *What is the strain at the UCS (assuming linear behavior)?* At the breaking limit the bone shortens by $\Delta L = (\mathrm{UCS}/Y)L_0$, which corresponds to a fractional shortening of $\Delta L/L_0 = \mathrm{UCS/Y}$. The femur shortens by $((170\,\mathrm{N/mm}^2)/(179 \times 10^2\,\mathrm{N/mm}^2))\,500\,\mathrm{mm} = (0.95\%)\,500\,\mathrm{mm} = 5\,\mathrm{mm}$ or 0.5 cm. This is a fractional decrease of $0.95\% \sim 1\%$, and a microstrain of 10,000 $\mu\epsilon$.

4.2.4 Energy Storage in Elastic Media

There are several essentially equivalent ways to determine the potential energy stored in elastic materials. From (4.1), in a spring the potential energy (PE) is

$$\mathrm{PE} = -\int_0^x F\,\mathrm{d}x' = \int_0^x kx'\mathrm{d}x' = \frac{1}{2}kx^2. \tag{4.11}$$

Changing to coordinates relative to the equilibrium position and changing the length to L gives

$$\mathrm{PE} = \frac{1}{2}k(L - L_0)^2. \tag{4.12}$$

Because $Y = kL_0/A, k = YA/L_0$, and $\epsilon = (L - L_0)/L_0$, we see that $L - L_0 = \epsilon L_0$. Therefore

$$\mathrm{PE} = \frac{1}{2}\frac{YA}{L_0}(\epsilon L_0)^2 = \frac{1}{2}(Y\epsilon^2)(AL_0) = \frac{1}{2}Y\epsilon^2 V, \tag{4.13}$$

where the volume $V = AL_0$. Because $\sigma = Y\epsilon$, this can be expressed as

$$\mathrm{PE} = \frac{1}{2}\sigma\epsilon V = \frac{1}{2}Y\epsilon^2 V = \frac{1}{2}\frac{\sigma^2}{Y}V. \tag{4.14}$$

The potential energy per unit volume PE/V is an intensive quantity.

This is equivalent to integrating

$$W = \int_{L_0}^{L} F\,\mathrm{d}L' = \frac{1}{2}F_{\mathrm{applied}}(L - L_0) = \frac{1}{2}k(L - L_0)^2 \tag{4.15}$$

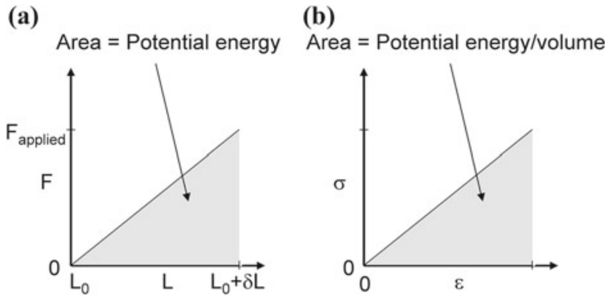

Fig. 4.13 Potential energy from area under **a** force–length and **b** stress–strain curves for a harmonic system

using $F_{\text{applied}} = k(L - L_0)$ or

$$W = \int_{L_0}^{L} F \, \mathrm{d}L' = \int_0^{\epsilon} (\sigma A) \, \mathrm{d}(\epsilon' L_0) = V \int_0^{\epsilon} \sigma \, \mathrm{d}\epsilon' = \frac{1}{2}\sigma\epsilon V, \tag{4.16}$$

where the last integral equals the area under the curve in Fig. 4.13 and can be obtained by replacing σ by $Y\epsilon$ and integrating to get $Y(\epsilon^2/2) = \sigma\epsilon/2$.

Designing Optimal Energy Storage Media

How can we design the best elastic storage medium for the body, such as would be desired for tendons? We would want (1) to store the maximum amount of potential energy for a given applied force F_{applied} and (2) the medium to withstand as large a F_{applied} as possible.

(1) The stored energy is

$$\mathrm{PE} = \frac{1}{2}\frac{\sigma^2}{Y} V = \left(\frac{(F_{\text{applied}}/A)^2}{2Y}\right) A L_0 = \frac{F_{\text{applied}}^2}{2Y}\frac{L_0}{A}, \tag{4.17}$$

so we would want to maximize the length L_0, minimize the cross-sectional area A, and minimize Y.

(2) However, to withstand a large F_{applied} we need to keep $\sigma = F_{\text{applied}}/A$ below the threshold for damage (which for tension is called the *ultimate tensile stress*, UTS), so we have a limit for how small we could make A to keep $\sigma \ll$ UTS. Also, there is a limit to how much the element can be lengthened $(L - L_0)$ for a large F_{applied}, given its motion requirements, such as that for a tendon. Because $L - L_0 = \epsilon L_0$, there are limits on how large both ϵ and L_0 can be. This sets a limit on the length L_0 and, because $\epsilon = \sigma/Y$, a limit on how small Y can be.

There is a tradeoff in the optimal values of L_0, A, and Y set by these two criteria. We want long and thin tendons with a small Y, but there are limits. In this design problem we also have to recognize that the medium, such as a tendon, is not perfectly harmonic or even elastic; all materials are really viscoelastic.

Energy Storage in Tendons and Long Bones

Let us return to the example of running in Fig. 3.34 [2]. The force on the Achilles tendon is 4,700 N. With a cross-sectional area of 89 mm^2, we see that $\sigma = 4,500\,\mathrm{N}/89\,\mathrm{mm}^2 = 53\,\mathrm{N}/\mathrm{mm}^2 = 53\,\mathrm{MPa}$. Given the maximum stress for tendons, the UTS, is $\sim 100\,\mathrm{N}/\mathrm{mm}^2 = 100\,\mathrm{MPa}$, during running the stress in these tendons is not far from the damage threshold. It is not surprising that the Achilles tendons of athletes occasionally snap, either partially or totally.

Using the stress–strain relation shown in Fig. 4.14, this stress leads to a strain of $0.06 = 6\%$. The length of the Achilles tendon is $L_0 = 250\,\mathrm{mm}$, so this strain corresponds to the tendon lengthening by 15 mm and

$$\mathrm{PE} = \frac{1}{2}\sigma\epsilon V = \frac{1}{2}\sigma\epsilon A L_0 = \frac{1}{2}(53\,\mathrm{N}/\mathrm{mm}^2)(0.06)(89\,\mathrm{mm}^2)(250\,\mathrm{mm}) \tag{4.18}$$

$$= 35,000\,\text{N-mm} = 35\,\text{N-m} = 35\,\mathrm{J}. \tag{4.19}$$

This is exactly the amount of energy we stated was being stored in the Achilles tendon during every step of a run.

How much energy is stored in the bones during this step? Let us examine the largest bone, the femur. We will use $L_0 = 0.5\,\mathrm{m} = 500\,\mathrm{mm}$ and $A = 330\,\mathrm{mm}^2$, and so $V = 165,000\,\mathrm{mm}^3$. Also $Y = 17,900\,\mathrm{MPa} = 17{,}900\,\mathrm{N}/\mathrm{mm}^2$. The upward

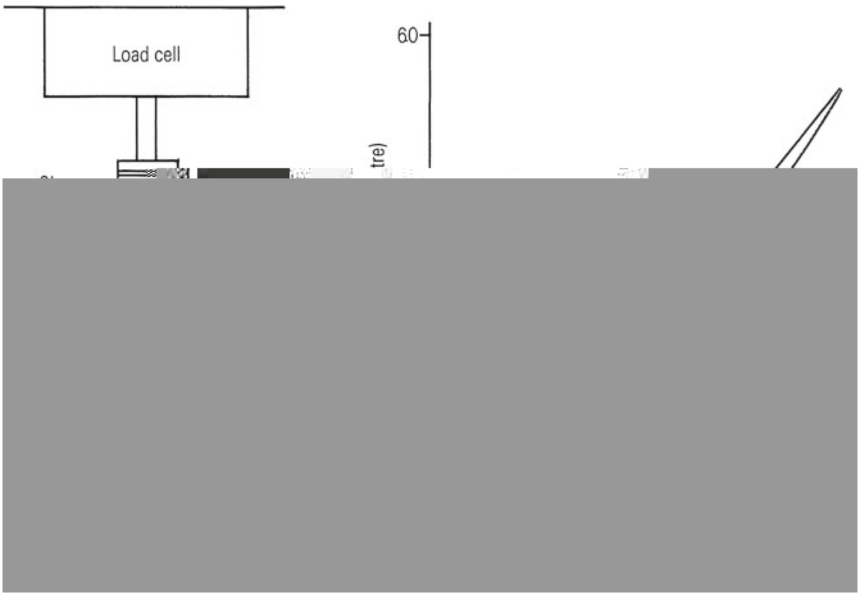

Fig. 4.14 Stress–strain (or force–length) for a human big toe flexor tendon, using the instrument on the *left*, with a 2-s-long stretch and recoil cycle. (From [2]. Copyright 1992 Columbia University Press. Reprinted with the permission of the Press)

normal force in Fig. 3.34 is 6,400 N, which we will assume is transmitted all the way to the femur. The stress is $6,400\,\mathrm{N}/330\,\mathrm{mm}^2 = 19.4\,\mathrm{N}/\mathrm{mm}^2$ and

$$\mathrm{PE} = \frac{1}{2}\frac{\sigma^2}{Y}V = \frac{1}{2}\frac{(19.4\,\mathrm{N}/\mathrm{mm}^2)^2}{17{,}900\,\mathrm{N}/\mathrm{mm}^2}\,165{,}000\,\mathrm{mm}^3 \tag{4.20}$$

$$= 1{,}730\,\mathrm{N\text{-}mm} = 1.73\,\mathrm{N\text{-}m} \sim 2\,\mathrm{J}. \tag{4.21}$$

If the same energy is stored in the tibia and fibula, then at most ∼3–4 J is stored in these long bones, which is a very small fraction of the 100 J kinetic energy lost per step.

Elastic energy recovery from tendons and ligaments may be important in motion, which means the energy storage is mostly elastic, it can be recovered in phase (which often means fast enough) to assist the motion, and failures due to stresses at high loading values and repetitive actions are not attained [66]. Longer tendons, such as Achilles tendons in the lower limb (∼120 mm long), can stretch more and tend to store more energy than shorter tendons (why?), but recoil and release the energy slower. These shorter tendons include the shoulder internal rotator muscle tendons used in throwing (∼58 mm) and the patellar tendon (∼48 mm). While the shorter tendons in the shoulder store less energy per tendon, there are many in parallel so much energy can still be stored in them and in shoulder ligaments, and with faster release.

4.3 Time-Independent Deviations in Hookean Materials

The Hookean (harmonic, linear) stress–strain relation is valid in tension and compression up to a limiting stress, corresponding to a strain $\ll 1$ that varies for different materials. Figure 4.15 shows a more realistic stress–strain relation. There is elastic Hookean behavior up to the point P, the *proportional limit*. The slope up to this stress is constant, the Young's modulus Y. The higher the Y, the *stiffer* or the less *compliant* the material (Fig. 4.16). At higher stresses, the stress–strain relation is nonlinear. Up to the *elastic limit*, denoted by $\mathrm{E_L}$, the object returns to its initial length when the stress is removed and there is no permanent deformation. In the linear and nonlinear elastic regimes, the stretched bonds relax totally and there is no rearrangement of atoms after the load is released.

For stresses beyond the elastic limit, there is *permanent or plastic deformation* and the length and shape of the object are different after the stress is removed. The *yield point or limit*, denoted by $\mathrm{Y_P}$, is at a stress somewhat higher than the elastic limit; above it much elongation can occur without much increase in the load. (Some do not distinguish between the elastic limit and the yield point.) Because it is often difficult to determine, the yield point is usually estimated by the intersection of the stress–strain curve with a line parallel to the linear part of the stress–strain curve, but with an intercept set at a strain of 0.2% (or 0.002). This offset method is illustrated in the inset in Fig. 4.15. The yield point occurs at the yield stress (or strength), YS.

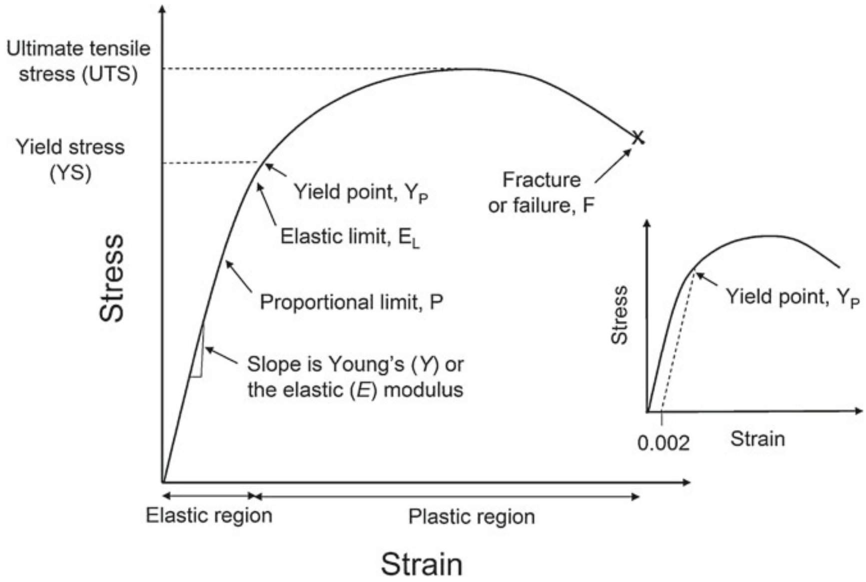

Fig. 4.15 General stress–strain relationship. The *engineering stress* is plotted here, which is the force divided by the initial area; it decreases after the UTS. The *true stress*, which is the force divided by the actual area increases after the UTS, due to the necking of the material. The inset shows the offset method to determine the yield point

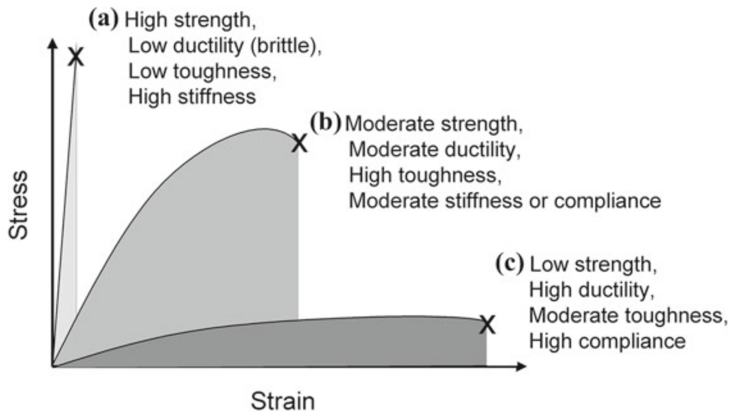

Fig. 4.16 Stress–strain curves of different types of materials with different levels of strength, ductility, and toughness. The engineering stress is plotted here. Strong materials fracture at very large ultimate tensile (or compressive) stress (UTS or UCS) (in Pa). Brittle materials have a small ultimate percent elongation (UPE) (unitless) and ductile materials have a large UPE. Tough materials can absorb much energy (when work is done on them) before they fracture, and so have a large work of fracture W_F (in J/m^2) or toughness, which is the shaded region under the stress-strain curve up to the point of fracture. Stiffer or less elastic materials have a larger Young's modulus Y (in Pa)

For tension, the material remains intact for larger stresses until the *ultimate tensile stress* (UTS), which is also called the *tensile strength* (TS) or, less commonly, the *tensile breaking strength* (TBS). The larger the breaking strength, the stronger is the material. Application of this stress leads to *fracture* at point F, which occurs at a strain called the *ultimate strain* or the *ultimate percent elongation* (UPE).

In Figs. 4.15 and 4.16, the actual type of stress being plotted is called the *engineering stress*. It is the force divided by the initial area, which is the area before any force is applied. Past the UTS, the engineering stress decreases as the material becomes narrower as it is pulled apart and the actual area becomes progressively smaller than this initial area, which is called "necking". (This narrowing is much, much more than that expected from the lateral strain, from Poisson's ratio.) The *true stress*, which is the force divided by the actual area, increases after the UTS, due to this necking.

Figure 4.17 shows that these stress–strain relations look qualitatively different for ceramics, metals, and elastomers because of their very different microscopic structures. Ceramics have a linear stress–strain relation with large slope Y. The fracture point appears only a little into the nonlinear elastic regime, and for smaller values of strain <0.1. To first order, bone (Fig. 4.18) is like a ceramic. (It is actually more complicated than that, as we will see.) Metals have a smaller Y, a larger nonelastic and plastic regime, and a larger UPE ~ 50 (in %). Elastomers (rubber, polymers) distort greatly even with small stresses because in this regime long, tangled chain molecules are straightened out at low stress in this *toe region* (the region of positive curvature at low strain, as in Fig. 4.25 below). The stress–strain curve is not linear. We will examine this again later. It takes much larger stresses to increase strain further after all of the chains have been straightened, because now bonds must be stretched. These materials have a very large UPE, typically >1. Blood vessels are elastomers.

There are striking differences in the plastic deformation regimes of the curves in Fig. 4.17. *Ductile* materials, such as modeling clay, chewing gum, plastic, and most metals, have an extensive plastic deformation phase (metals, elastomers, Fig. 4.17). *Nonductile* or *brittle* materials, such as glass, ceramics (stone, brick, concrete, pottery), cast iron, bone, and teeth, have a limited or essentially no plastic phase (ceramics, Fig. 4.17). They break easily when they are dropped; cracks easily propagate in them. The bonding in ductile materials allows layers of atoms to slip or shear past

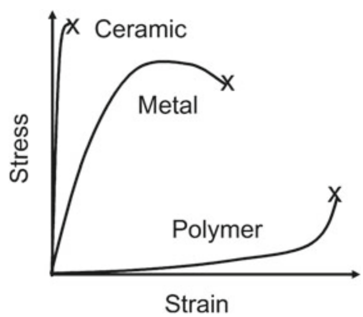

Fig. 4.17 Stress–strain curves for different types of materials under tension

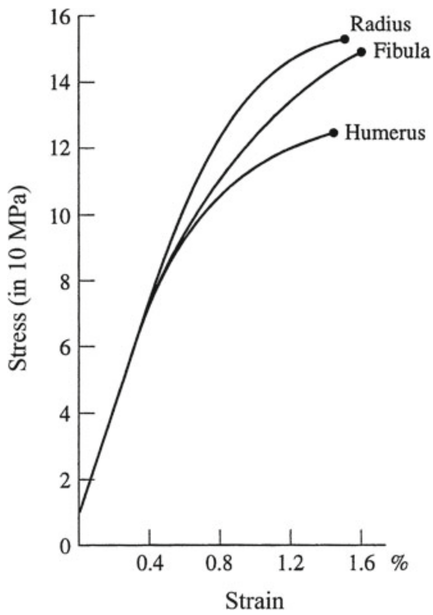

Fig. 4.18 Stress–strain curves under tension for wet limb bones of persons between 20 and 39 years of age. The *closed circles* are the fracture points. (From [6], based on [79])

each other, as in the bonding of metals. When thin rods of ductile materials are pulled at either end, they narrow in the center, forming a neck. In nonductile materials the covalent bonding is directional and does not permit this type of distortion. Typically, brittle materials have a small UPE and *ductile* materials have a large UPE.

Figures 4.15, 4.17, and 4.18 show the effects of tension. Under compression $\epsilon < 0$, and the stress–strain slope is the same Y for many conventional materials. For biological materials, like cartilage, they can be very different because of their complex nature. In cartilage, tension is resisted by the solid phase, while compression is resisted by the solid and liquid components. For ligaments and tendons, there is resistance to tension, but not to compression. For larger stresses the dependence is different even for many common nonbiological materials, and fracture occurs at the *ultimate compressive stress* (UCS), also called the *compressive strength* (CS) or the *compressive breaking strength* (CBS), which is different from the UTS in general (Table 4.1).

Table 4.1 gives the Y, UCS, and UTS for several types of materials. Note the very wide range of Y. Some ceramic-type materials, such as granite, porcelain, and concrete, can take much larger stresses in compression than in tension (UCS $\gg$ UTS). In others, UCS $<$ UTS. The two types of bones listed have a different porosity and very different properties. Compact bone, also known as cortical, or dense bone, has a large Young's modulus that is comparable to that of other strong materials (Fig. 4.18). It can withstand more stress in compression than in tension, but unlike the ceramics it has a fairly large UTS. Trabecular bone, also known as spongy or cancellous bone, is more porous and has a very small Y, almost as small as that of rubber (Fig. 4.19a).

Table 4.1 Mechanical properties of common materials

Material	Y ($\times 10^3$ MPa = GPa)	UCS (MPa)	UTS (MPa)
Hard steel	207	552	827
Rubber	0.0010	–	2.1
Nylon 66	1.2–2.9	–	59–83
Gold	78	–	–
Tungsten	411	–	–
Granite	51.7	145	4.8
Concrete	16.5	21	2.1
Southern Pine (select structural)[a]	11	25	19
Southern Pine (No. 2 grade)[a]	10	20	10
Oak	10.0	59	117
Fused quartz	73	–	69
Diamond	965	–	–
Porcelain	–	552	55
Alumina (85% dense)	220	1,620	125
Alumina (99.8% dense)	385	2,760	205
Compact bone	17.9	170	120
Trabecular bone	0.076	2.2	–

[a] Standard and utility Southern Pine can have lower Y and much lower UCS and UTS than these construction grades. Other types of pine will have different values also
Using data from [10, 29, 31, 74]

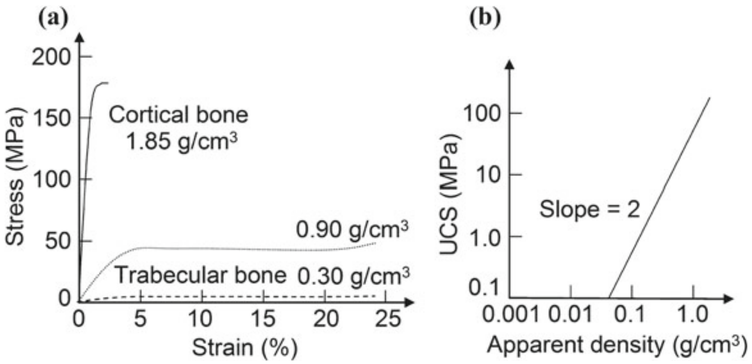

Fig. 4.19 Mechanical properties of bone as a function of apparent density. **a** Stress–strain of different densities of bones under compression. **b** UCS of trabecular bone versus bone density. (Based on (**a**) [24, 38], and (**b**) [4, 38])

Typical stress–strain curves for structural materials in the body under tension are shown in Fig. 4.20. Yamada [79] has published extensive measurements of stress–strain relations for many components of the human body. Table 4.2 lists several elastic constants determined from these data. Fig. 4.21 shows one series of these

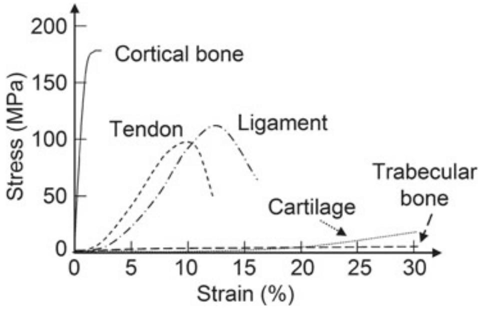

Fig. 4.20 Typical stress–strain of cortical and trabecular bone, cartilage, ligaments, and tendons under tensile loading. For some structural materials, the stress–strain relations are very different for different types of the material, such as for cartilage. (Based on [4, 79])

stress–strain relations, for different sections of the small intestine. Note that these curves are very nonlinear for a given stress, as are many soft human tissues [7, 28, 51]; this is discussed more below.

To first order, bones, teeth, and nails, all hard materials, have similar stress–strain curves that are ceramic-like. Tendons, cartilage, resting muscle, skin, arteries, and intestines all have more elastomer-like properties because they have much more collagen; they are really non-Hookean materials. This is also seen in Fig. 4.20. Each of these body materials has viscoelastic properties, as we will address below.

Compact bone in different long bones in the human body has slightly different properties (Table 4.6 below). These properties can be *anisotropic* (Fig. 4.22, Table 4.3), meaning that the properties are different along different directions. For example, this is true of bone and of the esophagus and small intestine, which are composed of very different materials. The small intestine stretches much more easily in the transverse direction than the longitudinal direction, as seen in Fig. 4.21 [7, 28, 51]. Many biological materials are anisotropic, as are many common materials, such as wood due it is grain structure. Some materials are fairly *isotropic*.

Several elastic properties vary with age. These properties also change with density, which is a main reason why people with *osteoporosis* often fracture bones during a fall. Figure 4.19b shows the UCS decreases roughly as the square of bone density. (These changes with age are, in part, linked to such changes in density and the thinning of the bones. When your long bones are thicker due to heavy physical activity in childhood and adolescence, the chance for fracture decreases even with the loss of density [42]. Exercise that loads the long bones, can slow decreases in bone porosity and thickness with advancing age [30].) Fig. 4.23 shows that the mechanical properties of soft tissues, in this case the anterior cruciate ligament (ACL) in the knee, also depend on age, as well as direction (also see Fig. 4.21.)

Material properties in the body change with time for reasons aside from aging and injury. The tissue in the cervix softens during pregnancy, with the modulus (measured at $\sim$20% strain) being $\sim$0.1–1 MPa before and during the early stages of pregnancy, to contain the fetus well, and decreasing to $\sim$1–10 kPa at term (beyond 37 weeks of gestation), to enable expansion and easy delivery [53]. (This modulus is technically the tangent modulus of elasticity, which is defined later this chapter.)

Table 4.2 Elastic properties of organs under tension (human, unless otherwise specified)

Organ	UTS (MPa)	UPE (%)	Y (MPa)
Hair (head)	197	40	12,000
Dentin (wet teeth) (compression)	162	4.2	6,000
Femoral compact bone (compression)	162	1.8	10,600
Femoral compact bone	109	1.4	10,600
Tendons (calcaneal = Achilles)	54	9.0	250
Nail	18	14	160
Nerves	13	18	10
Intervertebral disc (compression)	11	32	6.0
Skin (face)	3.8	58	0.3
Vertebrae	3.5	0.8	410
Elastic cartilage (external ear)	3.1	26	4.5
Hyaline cartilage (synovial joints)	2.9	18	24
Intervertebral disc	2.8	57	2.0
Cardiac valves	2.5	15	1.0
Ligaments (cattle)	2.1	130	0.5
Gall bladder (rabbit)	2.1	53	0.05
Umbilical cord	1.5	59	0.7
Vena cava (longitudinal direction)	1.5	100	0.04
Wet spongy bone (vertebrae)	1.2	0.6	200
Coronary arteries	1.1	64	0.1
Large intestine (longitudinal direction)	0.69	117	0.02
Esophagus (longitudinal direction)	0.60	73	0.03
Stomach (longitudinal direction)	0.56	93	0.015
Small intestine (longitudinal direction)	0.56	43	0.2
Skeletal muscle (rectus abdominis)	0.11	61	0.02
Cardiac muscle	0.11	64	0.08
Liver (rabbit)	0.024	46	0.02

The Young's modulus is given in the low strain limit
Determined using [79]

We have seen that materials in the body are sometimes composed of different structures (i.e., they are composite materials), are anisotropic, and are sometimes layered. Moreover, a given material in a given organ or part of the body can also be very nonuniform. One example is seen in our teeth. Teeth are composed of pulp, which is mostly surrounded by dentin, which itself is overlayed by enamel. The enamel is very stiff and hard, and has very nonuniform properties [44]. Near the surface of the tooth (the occlusal surface), of say the second molar, the Young's modulus approaches 120 GPa, and it decreases to approximately 55 GPa near the enamel–dentine surface. It is also somewhat larger on the lingual (tongue) side than the buccal (cheek) side.

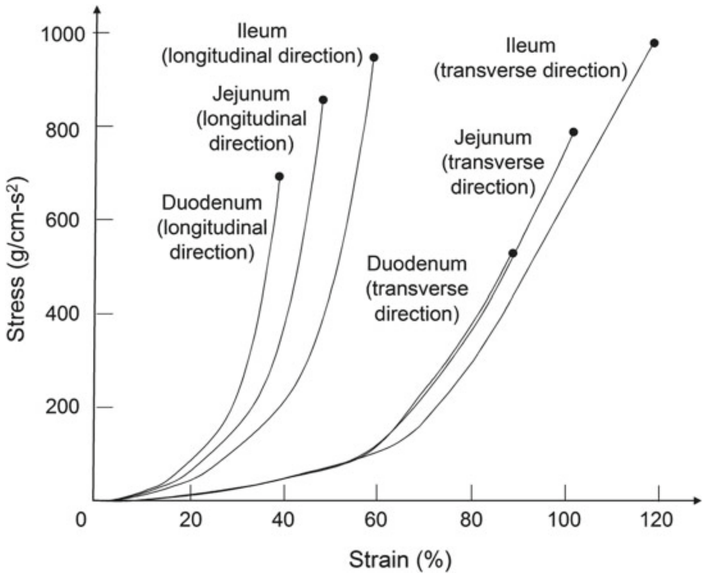

Fig. 4.21 Stress–strain curves for material in different sections of the small intestine of persons from 20 to 29 years of age, under tension in the longitudinal and transverse directions. The *closed circles* are the fracture points. (Based on [79])

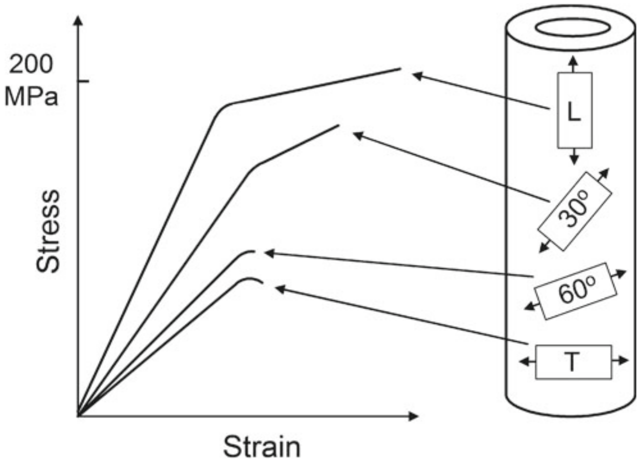

Fig. 4.22 Anisotropic properties of cortical bone specimens from a human femoral shaft tested under tension. Each curve ends at its point of failure. (Based on [23, 24])

Table 4.3 Mechanical properties of human cortical bone

Young's modulus, Y (GPa)	
Longitudinal	17.4
Transverse	9.6
Bending	14.8
Shear modulus (GPa)	3.51
Poisson's ratio	0.39
Yield stress (MPa)	
Tensile—longitudinal	115
Compressive—longitudinal	182
Compressive—transverse	121
Shear	54
Ultimate stress (MPa)	
Tensile—longitudinal	133
Tensile—transverse	51
Compressive—longitudinal	195
Compressive—transverse	133
Shear	69
Bending	208.6
Ultimate strain	
Tensile—longitudinal	0.0293
Tensile—transverse	0.0324
Compressive—longitudinal	0.0220
Compressive—transverse	0.0462
Shear	0.33
Bending	(0.0178 bovine)

Using data from [45]

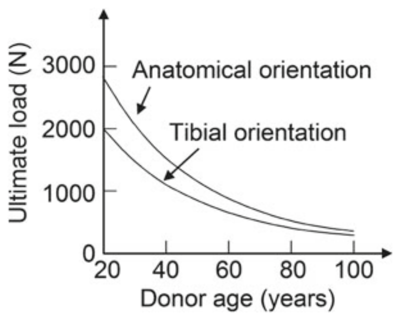

Fig. 4.23 Age variation of the ultimate load (UTS) of human anterior cruciate ligament (ACL) as a function of age and orientation. (Based on [4, 78])

What is the strongest part of the body? If we were to define strength as the largest UTS, then of the body components in Table 4.2 it is not bone and not dentin in the teeth, but hair. (Of course, if we were to include tooth enamel, which is not in this table, it would beat out hair for this distinction. It is the hardest biological material in the body.)

4.3.1 Non-Hookean Materials

Many body materials cannot be modeled as Hookean springs, even for small stresses. This is typically true for collagenous tissues, such as tendons, skin, mesentery (which are the folds attaching the intestines to the dorsal abdomen), the sclera, cartilage, and resting skeletal muscle. Experimentally, for resting muscles and the materials shown in Fig. 4.21 it is found that for larger strains

$$\frac{\mathrm{d}\sigma}{\mathrm{d}\epsilon} = \alpha(\sigma + \beta). \tag{4.22}$$

This is very different than that for materials such as bone for which $\sigma = Y\epsilon$, with a $\mathrm{d}\sigma/\mathrm{d}\epsilon = Y$ that is independent of stress. Instead they are characterized by the slope of the stress-strain curve, $\mathrm{d}\sigma/\mathrm{d}\epsilon$, which is called the *tangent modulus of elasticity*, which is a function of stress or strain, as in (4.22).

Equation (4.22) can be integrated after bringing the σ and ϵ terms to opposite sides of the equation

$$\frac{\mathrm{d}\sigma}{\sigma + \beta} = \alpha\ \mathrm{d}\epsilon \tag{4.23}$$

$$\ln(\sigma + \beta) = \alpha\epsilon + \gamma, \tag{4.24}$$

where γ is a constant. Exponentiating both sides gives

$$\sigma + \beta = \exp(\alpha\epsilon)\exp(\gamma) \qquad \text{and} \qquad \sigma = \mu \exp(\alpha\epsilon) - \beta, \tag{4.25}$$

where $\mu = \exp(\gamma)$. Because $\sigma(\epsilon = 0) = 0$, we see that $\beta = \mu$ and so

$$\sigma = \mu(\exp(\alpha\epsilon) - 1). \tag{4.26}$$

This is illustrated in the passive curves in Fig. 5.21. (See Appendix C for more information about this method of solution.)

Sometimes the Lagrangian strain $\lambda = L/L_0 = \epsilon + 1$ is defined, where L is the length and L_0 is the length with no stress. Equation (4.26) becomes

$$\sigma = \mu' \exp(\alpha\lambda) - \mu = \mu' \exp(\alpha L/L_0) - \mu, \tag{4.27}$$

with $\mu' = \mu \exp(-\alpha)$.

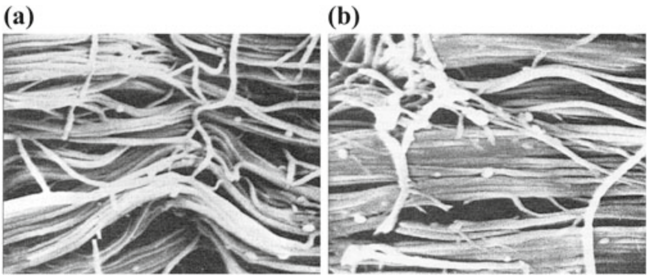

Fig. 4.24 Scanning electron micrographs (10,000×) of **a** unloaded and **b** loaded collagen fibers from human knee ligaments, showing them straightening out under the tensile load. (From [39]. Used with permission)

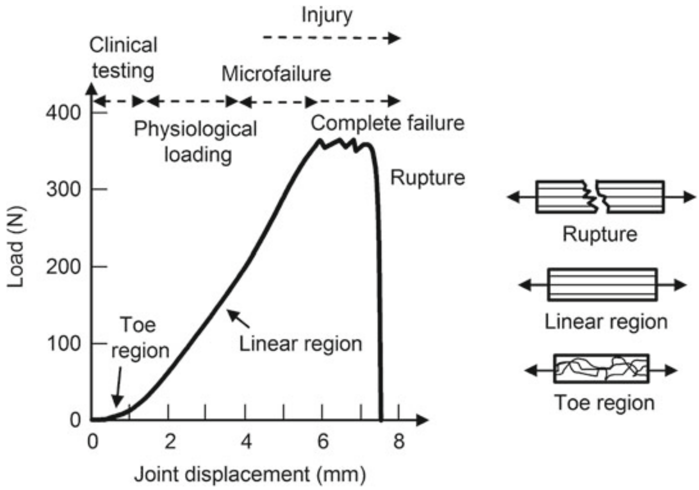

Fig. 4.25 Force–deformation curve for an ACL (ligament), showing regimes of clinical test loading, loads during physiological activity (toe and linear regions), and loads leading to microfailure and ultimate rupture and complete failure. (Based on [58, 60])

At larger strains this exponential form may not work well. In the *neo-Hookean* regime, finite strain, $E = \frac{1}{2}(\lambda^2 - 1)$, is defined, which for small deformations approaches the small-strain approximation, $\epsilon = \lambda - 1$. Soft, neo-Hookean materials tend to follow a linear relationship between stress and λ^2 (or E), and not a linear or exponential relationship between stress and λ (or ϵ). This neo-Hookean regime and other more general ways to define strain are described in Problems 4.20–4.22.

Such non-Hookean stress–strain curves are typical for materials with fibers. As mentioned earlier, there are large strains for small stresses where the tangled fibers are being aligned (in this toe regime), but much larger stresses are required to achieve much higher strains where the already-aligned fibers are being stretched (Fig. 4.24). Try this by stretching yarn. The fibers begin to tear at the UTS, corresponding to the load seen in Fig. 4.25.

For tendons (Fig. 4.14) and ligaments (Fig. 4.25) the tangent modulus of elasticity increases with strain at low strain (in the toe region) and then becomes constant (in the linear region) until it ruptures (and so, before rupture it is not well described by (4.22)). For tendons, the linear regime begins when they are stretched ∼2% (range from 1.5–4%) or stressed to ∼16 MPa (5–30 MPa), and in the linear regime the tangent modulus is ∼1.2 GPa (0.6–1.7 GPa) [80].

We will now return to the deformation of Hookean materials, like bone. We will revisit the properties of these non-Hookean materials in the discussions of viscoelasticity and muscles.

4.4 Static Equilibrium of Deformable Bodies (Advanced Topic)

We now examine the deformation of bones under the action of forces in more detail. We have seen how they can be pulled (tension) and squeezed (compression); now we will see how they can bend. This analysis will help us understand how bones fracture when they are bent, such as during slipping and skiing accidents. We will also learn why long bones, like the femur, are strong even though they are hollow. As an added benefit, we will derive a scaling law that will help us understand some aspects of metabolism.

Physics classes usually describe the motion of point objects or more extended objects that never deform. However, no object is a point and objects do deform. Such extended objects are treated in great detail in mechanical and civil engineering curricula for obvious reasons. We will examine how such finite bodies bend to understand bone fracturing better, and will follow the treatment of [6]. The derivations in this section can be treated as a more advanced topic. They can be skipped and the final results can be used.

Let us consider the beam of length L shown in Fig. 4.26. It has a constant cross-section throughout its length; the cross-section need not be rectangular or circular. It is supported at both ends and a force F is applied to the center at the top as shown. We expect the beam to bend. For beams composed of most materials, we expect it to

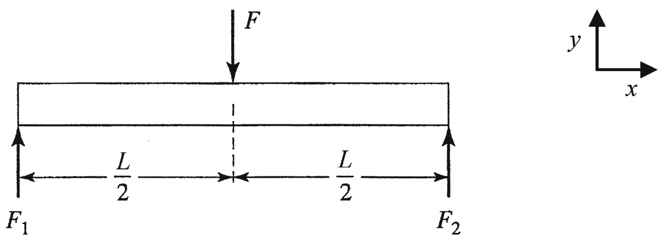

Fig. 4.26 Force diagram of a rectangular beam with a force applied to the *middle*. (From [6])

bend to a shape with a top surface that is somewhat cylindrical, and have a circular arc cross-section in the plane of the paper. If this were a rubber band, we would expect a more triangular deformation. Because we want to learn about bones, we anticipate some small degree of bending.

In this two-dimensional problem, in equilibrium $\sum F_x = 0$, $\sum F_y = 0$, and $\sum \tau_z = 0$ (2.8) for the entire beam. There are no forces in the x direction. We are assuming that in the equilibrium bent position, the amount of bending is small, so nothing interesting is happening in the x direction. The downward force F (which is the negative y direction) that is applied to the center of the beam is countered by the forces $F/2$ at the two supports, as is shown. The total torques on this beam are zero about any axis.

So far, this is how we treated the statics of rigid bodies in Chap. 2. Now let us examine the static equilibrium for only a part of the beam. As seen in Fig. 4.27, we consider the right side of the beam, from the right end to a distance x to the left of this end. The three equilibrium conditions also apply to this section, as well as to any other section. We can again ignore the x direction because there are no forces in that direction. For this example, with $x < L/2$ for now, there is apparently only one force acting on this piece of the beam, the upward force $F/2$ at the right support. This force also causes a torque and so

$$\sum F_y = \frac{1}{2}F \quad \text{and} \quad \sum \tau_z = \frac{1}{2}xF. \tag{4.28}$$

We have chosen the torque axis normal to the page at the left end of this portion of the beam (at a distance x from the right end). Because this portion of the beam is static, both terms must sum to zero. Something is wrong. What? We have excluded the force on this section from the other part of the beam. These internal forces must be $-F/2$ to balance the effect of the external force $F/2$ (Fig. 4.28). This "internal vertical force," often called the "internal shear force" or just the "shear force," supplied at the border with the other section is similar to the "normal" or "reaction" force felt by an isolated part of the body, as that on the leg from the hip. There must also be an internal torque applied by the other part of the beam equal to $-xF/2$. This "internal torque" is also called the "internal bending moment" or just the "bending moment."

For longer sections, with $L/2 < x < L$, the section feels the upward force at the right support $F/2$ and also the applied force $-F$ at the center. Both lead to torques. Excluding internal forces and torques

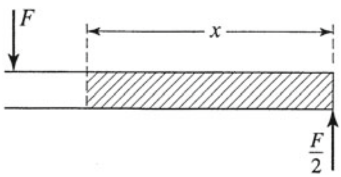

Fig. 4.27 External forces on a section of a beam. (From [6])

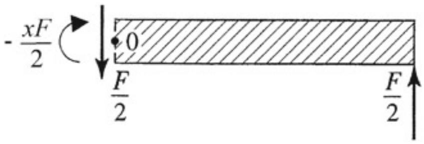

Fig. 4.28 Internal (*left*) and external (*right*) forces on an isolated section of the lined portion of the beam in Fig. 4.27. This is a free-body diagram of this portion. (From [6])

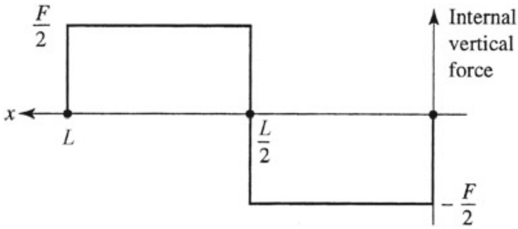

Fig. 4.29 Internal vertical force for a right-adjusted section in the beam. (From [6])

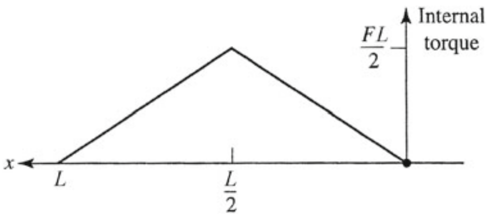

Fig. 4.30 Internal torque for a right-adjusted section in the beam. (From [6])

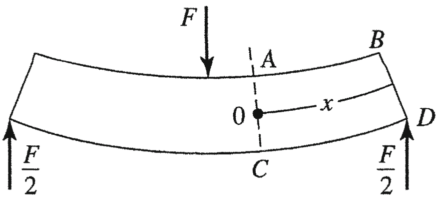

Fig. 4.31 Bending of a loaded beam. (From [6])

$$\sum F_y = -\frac{1}{2}F \quad \text{and} \quad \sum \tau_z = \frac{1}{2}(L-x)F \tag{4.29}$$

and so the internal force is $F/2$ and the internal torque is $-(L-x)F/2$. The internal vertical force and torque are plotted versus x in Figs. 4.29 and 4.30. When we include these internal forces and torques, each portion of the beam is in static equilibrium. For now assume that $x < L/2$; extension to $L/2 < x < L$ is straightforward.

How do the internal torques arise? With the applied force, the beam deforms to that in Fig. 4.31 (in which the deformation is greatly exaggerated for a long bone). Clearly, the top portion is compressed and has a length $<L$, while the bottom portion is under tension and has a length $>L$. (This should become clearer if you take a spring or Slinky™ and bend it into a circular arc.) Somewhere in the middle (in the y direction) there is no compression or tension, so the length in this neutral axis is L.

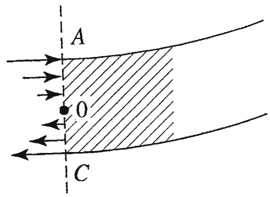

Fig. 4.32 Internal stresses in a bent beam. (From [6])

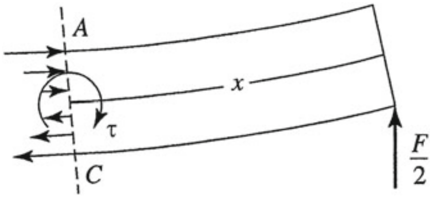

Fig. 4.33 Torques in a bent beam. (From [6])

(The neutral axis is in the center (in the y direction) for symmetrical cross-sections.) For the top to be compressed there must be an internal force at the top in the $+x$ direction pushing into the section from the other portion (Fig. 4.32). Similarly, for the bottom to be under tension there must be an internal force at the bottom in the $-x$ direction, pulling into the section from the other portion. As shown in this figure, there is a smooth variation of this force from the top (called point A) to the bottom (point C), with it being zero at the neutral axis (point O). Clearly, the sum of these internal forces in the x direction must be zero.

Each of these internal forces causes a torque in the z direction, $-F_I y_I$, and each of these leads to a clockwise, or negative, torque about point O (Fig. 4.33). With forces to the right called positive, clearly $F_{\mathrm{A}} > 0$ and $F_{\mathrm{C}} < 0$, and with $y_{\mathrm{A}} > 0$ (measured upward from the neutral axis) and $y_{\mathrm{C}} < 0$, we find that the torque contributions from points A and C, $-F_{\mathrm{A}} y_{\mathrm{A}}$ and $-F_{\mathrm{C}} y_{\mathrm{C}}$, are equal in symmetrical situations. We can sum all of these internal torques to arrive at τ_{internal}, and then

$$\sum \tau_z = \tau_{\text{internal}} + \frac{1}{2} F x = 0 \tag{4.30}$$

for static equilibrium.

What is the total internal torque? Consider a beam with arbitrary, but constant, cross-section, as shown in Fig. 4.34. The distance up from the neutral axis (with point O') is y, and there is a cross-section element with area $\mathrm{d}A$ at this position; $\mathrm{d}A = w(y)\mathrm{d}y$, where $w(y)$ is the width at y. There is a force acting on this area element at height y, which is

$$\mathrm{d}F(y) = \sigma(y)\mathrm{d}A(y). \tag{4.31}$$

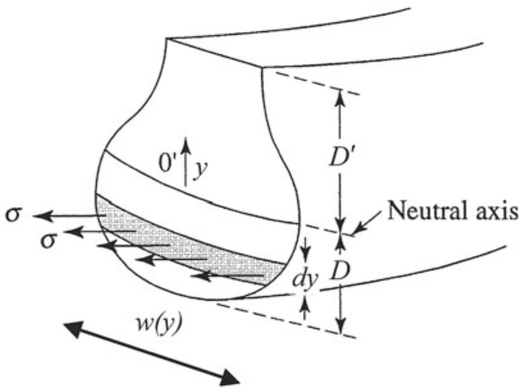

Fig. 4.34 Stress in a bent beam versus position. An area element (for $y < 0$) is shown as a shaded region, with area $\mathrm{d}A = w(y)\mathrm{d}y$ for width $w(y)$. (From [6])

For each element there is a torque

$$-y\,\mathrm{d}F = -y\sigma(y)\mathrm{d}A(y). \tag{4.32}$$

So the total internal torque is

$$\tau_{\text{internal}} = -\int_{y_\mathrm{B}}^{y_\mathrm{A}} y\sigma(y)\mathrm{d}A(y) = -\frac{1}{2}Fx, \tag{4.33}$$

where $y_\mathrm{A} = D'$ and $y_\mathrm{B} = -D$ in Fig. 4.34. (The dA element includes the dy term.)

What is the distribution of σ? To first order, the beam deforms to a circular arc (Figs. 4.35 and 4.36) of radius R and angle α. At the midline neutral axis, where $y = 0$, we see that $L = R\alpha$ for $\alpha \ll 1$ and so $\alpha = L/R$. If the beam has a thickness in the y direction of d and the beam is symmetrical, then the top of the beam is $(R - d/2)\alpha$ long and the bottom is $(R + d/2)\alpha$ long. In general,

$$L(y) = (R - y)\alpha = (R - y)\frac{L}{R} = \left(1 - \frac{y}{R}\right)L, \tag{4.34}$$

so the elongation is $L(y) - L = -(y/R)L$ and the strain is

$$\epsilon(y) = -\frac{y}{R}, \tag{4.35}$$

where $1/R$ is the curvature.

In the harmonic region, with $\sigma = Y\epsilon$, the stress would be expected to be $-Y(y/R)$. Given the direction of the forces shown in Fig. 4.34, the stress is defined to be positive for positive y, so

$$\sigma(y) = Y\frac{y}{R}. \tag{4.36}$$

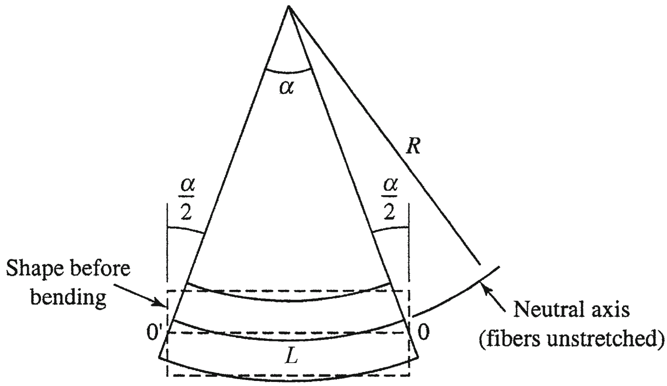

Fig. 4.35 Geometry of a bent beam. (From [6])

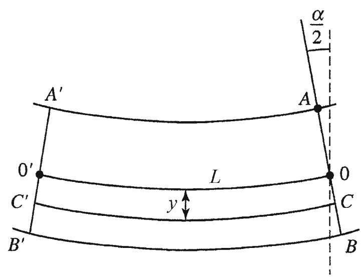

Fig. 4.36 Geometry of a bent beam in more detail. (From [6])

4.4.1 Bending of a Beam (or Bone)

The total internal torque is

$$\tau_{\text{internal}} = -\int_{y_B}^{y_A} y\left(Y\frac{y}{R}\right)\mathrm{d}A(y) = -\frac{Y}{R}\int_{y_B}^{y_A} y^2\mathrm{d}A(y) = -\frac{1}{2}Fx, \tag{4.37}$$

where $y_A = d/2$ and $y_B = -d/2$ for the symmetrical situation.

The *area moment of inertia* is defined as

$$I_A = \int_{y_B}^{y_A} y^2\mathrm{d}A(y). \tag{4.38}$$

(This parameter is very different than the moment of inertia defined in (3.24). This one sums the squares of the distances from a plane, while the other and more usual one sums the squares of the distances from an axis.) Using this moment and the definition of the bending moment M_B due to applied forces ($M_B = -Fx/2$ at equilibrium), (4.38) is

$$M_{\mathrm{B}} = -\frac{Y}{R}\, I_{\mathrm{A}} \tag{4.39}$$

and the magnitude of the curvature is

$$\frac{1}{|R|} = \frac{|M_{\mathrm{B}}|}{Y I_{\mathrm{A}}}. \tag{4.40}$$

Equations (4.39) and (4.40) interrelate four quantities (1) the applied forces, through M_{B}; (2) the intensive materials properties, through Y; (3) the physical deformation (response) of the beam due to the applied forces, through R; and (4) the shape of the object, through I_{A}.

For a given M_{B} and Y, when the area moment of inertia I_{A} is large there is little bending, while when I_{A} is small there is much bending. For example, the area moment of inertia for a rectangle of height h and width w is

$$I_{\mathrm{A}} = \int_{-h/2}^{h/2} y^2 (w\mathrm{d}y) = \frac{1}{12} w h^3, \tag{4.41}$$

where $\mathrm{d}A = (w)\mathrm{d}y$. Consider a 2×6 cm rectangle arranged vertically (see Fig. 4.37) with $w = 2$ cm and $h = 6$ cm. It has an $I_{\mathrm{A}} = 2\,\mathrm{cm} \times (6\,\mathrm{cm})^3/12 = 36\,\mathrm{cm}^4$. If this same rectangle were horizontal, then $w = 6$ cm and $h = 2$ cm, and $I_{\mathrm{A}} = 6\,\mathrm{cm} \times (2\,\mathrm{cm})^3/12 = 4\,\mathrm{cm}^4$. For the same M_{B} and Y, the horizontal beam would bend $9\times$ more. Try this with a yardstick!

The moment I_{A} is larger when the mass is distributed far from the central action, and there is less bending for a given bending moment when this occurs. This illustrates why "I beams" are used in construction instead of solid beams with the same overall rectangular cross-section (Fig. 4.38). The mass far from the neutral axis provides the resistance to bending, which is proportional to I_{A}, and the lack of material near the neutral axis lowers the weight of the beam.

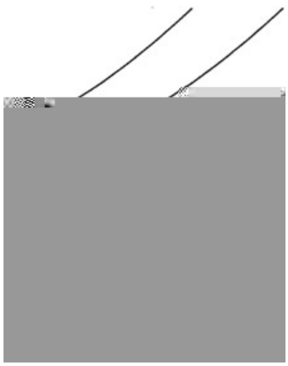

Fig. 4.37 Geometry for calculating the area moment of inertia for a rectangular beam. The same calculation can be used for the very different rectangular beam, with $h < w$. (From [6])

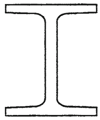

Fig. 4.38 An I-beam. (From [6])

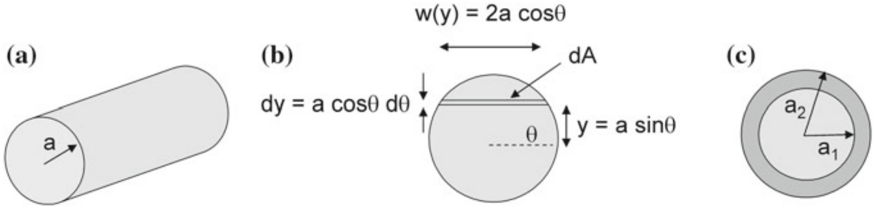

Fig. 4.39 **a** A solid circular beam; **b** determining the area moment of inertia for a solid circular cylinder beam; **c** a hollow circular beam

Why Long Bones Are Hollow

We now see why the long bones in the body can be hollow with much loss of weight and little loss of stiffness. The mass far from the neutral axis provides resistance to bending, while that near the neutral axis contributes little. Such hollow bones have sufficient resistance to bending, as well as larger resistance to bending per unit mass than do solid bones.

The area moment of inertia for a solid circular beam of radius a (Fig. 4.39a) is given from (4.38) $I_{\mathrm{A,solid}} = \int_{-a}^{a} y^2 \mathrm{d}A(y)$. Using Fig. 4.39b, we see that $y = a\sin\theta$, $\mathrm{d}y = a\cos\theta\,\mathrm{d}\theta$, and $w(y) = 2a\cos\theta$, so $\mathrm{d}A = 2a^2\cos^2\theta\,\mathrm{d}\theta$. Therefore

$$I_{\mathrm{A,solid}} = \int_{-\pi/2}^{\pi/2} (a\sin\theta)^2(2a^2\cos^2\theta\,\mathrm{d}\theta) = 2a^4\int_{-\pi/2}^{\pi/2}\sin^2\theta\cos^2\theta\,\mathrm{d}\theta = \frac{1}{4}\pi a^4, \tag{4.42}$$

because $\sin^2\theta\cos^2\theta = \sin^2\theta(1-\sin^2\theta) = \sin^2\theta - \sin^4\theta$, and $\int_{-\pi/2}^{\pi/2}\sin^2\theta\,\mathrm{d}\theta = \pi/2$ and $\int_{-\pi/2}^{\pi/2}\sin^4\theta\,\mathrm{d}\theta = 3\pi/8$. The mass of the solid circular beam with length L and mass per unit volume (mass density) ρ is $M_{\mathrm{solid}} = \rho\pi a^2 L$. Using (4.42), it is clear that for a hollow circular beam with hollow radius a_1 and total radius a_2 (Fig. 4.39c),

$$I_{\mathrm{A,hollow}} = \frac{\pi(a_2^4 - a_1^4)}{4} \tag{4.43}$$

and $m_{\mathrm{hollow}} = \rho\pi(a_2^4 - a_1^4)L$. Table 4.4 shows that only 6% of the bending stiffness is lost with $a_1/a_2 = 0.5$, even though there is a 25% decrease in mass. For a beam of radius a and thin wall of thickness $w \ll a$ ($a_2 = a$, $a_1 = a - w$), we find that $I_{\mathrm{A,hollow}} = \pi a^3 w$, $m_{\mathrm{hollow}} = 2\rho\pi a w L$, and $I_{\mathrm{A,hollow}}/m_{\mathrm{hollow}} = a^2/2\rho L$. While the resistance to bending per unit mass increases as the beam (or bone) becomes more

Table 4.4 Comparison of area moments of inertia and masses of hollow and solid circular beams

a_1/a_2	$I_{A,\text{hollow}}/I_{A,\text{solid}}$	$m_{\text{hollow}}/m_{\text{solid}}$	$(I_{A,\text{hollow}}/m_{\text{hollow}})/(I_{A,\text{solid}}/m_{\text{solid}})$
0	1.0	1.0	1.0
0.2	0.998	0.96	1.04
0.4	0.974	0.84	1.16
0.5	0.937	0.75	1.25
0.6	0.870	0.64	1.36
0.8	0.590	0.36	1.64
0.9	0.344	0.19	1.81

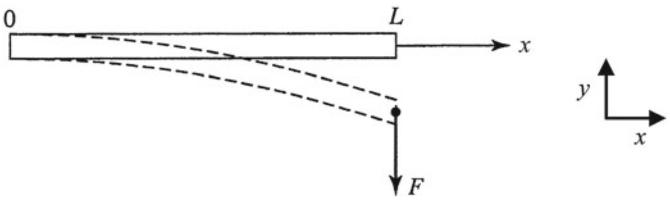

Fig. 4.40 Bending of a cantilever beam loaded at one end. (From [6])

Fig. 4.41 Bending moment at end point x along the axis for the loaded cantilever beam. (From [6])

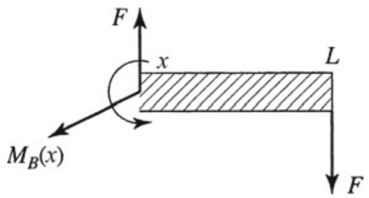

and more hollow, there is a limit to how much smaller I_A can become with smaller w before the beam can bend too much; it can also buckle (see below).

Bone Bending and Scaling Relationships

Let us consider a cantilever of length L that is firmly attached at the left and initially free at the right side (Fig. 4.40). A force F is applied downward at this free end. *How much does this end bend down?* For every section of length x (from the right), there is an applied moment $M_B(x) = F(L - x)$ (Figs. 4.41 and 4.42). Locally, at each x there is a curvature $1/R$, given by (4.40). The local curvature of any curve (in this case the beam) can be expressed by $\mathrm{d}^2y/\mathrm{d}x^2 = -1/R(x)$ and so

$$\frac{\mathrm{d}^2 y}{\mathrm{d}x^2} = -\frac{F(L-x)}{YI_A}. \tag{4.44}$$

At the wall ($x = 0$) the position is fixed, so $y = 0$ and $\mathrm{d}y/\mathrm{d}x = 0$ at $x = 0$.

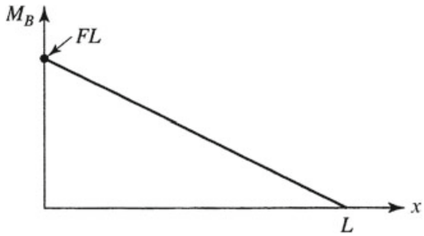

Fig. 4.42 Moment versus x for the loaded cantilever beam. (From [6])

Integrating (4.44) twice and applying these conditions gives the downward deflection at each x

$$y(x) = -\frac{F}{6YI_\mathrm{A}}((L-x)^3 + L^2(3x-L)). \tag{4.45}$$

(See Appendix C for more information about the solution.) At the end

$$y(L) = -\frac{FL^3}{3YI_\mathrm{A}}. \tag{4.46}$$

We will use this relation in the discussion about scaling in metabolism in Chap. 6.

4.5 Time-Dependent Deviations from Elastic Behavior: Viscoelasticity

So far we have asked how large of a force is needed to create a given strain or to break a bone. We have never asked whether it makes a difference if this force were applied quickly or slowly. (If we were to ask this, we would really need to know if it were applied fast or slow relative to a defined time scale.) The responses of most materials inside or outside the body depend on these temporal dependences and on history, to some degree. This very important type of mechanical behavior is called *viscoelasticity*. Biological liquids and solids are usually viscoelastic, and this includes tendons, ligaments, cartilage, bone, and mucous. We will see how to model the viscoelasticity of body materials, and how it affects us—such as in fractures and collisions [22, 27].

Perfectly harmonic elastic behavior is modeled by a spring (Fig. 4.43a), with

$$F(t) = kx(t), \tag{4.47}$$

where F is now the applied force and x is the response, which is the displacement of the end of the spring. k is the spring constant. The force and displacement depend on the current state at the current time t and are independent of history.

Fig. 4.43 **a** Ideal (or perfect) spring and **b** ideal (or perfect) dashpot. These are the two basic building blocks used in modeling the mechanical response of materials

Perfectly viscous behavior is modeled by a *dashpot* (Fig. 4.43b), with

$$F(t) = cv(t) = c\frac{\mathrm{d}x(t)}{\mathrm{d}t}, \tag{4.48}$$

where the response depends on the speed. c is a constant that describes damping due to viscosity. (In the biomedical engineering community this is sometimes called η.) An idealized dashpot is a piston moving in a cylinder, impeded by its movement in a viscous fluid. The displacement of the piston in the dashpot depends on its history! (The damping motion of a screen door closer can be modelled as a dashpot.) This viscosity damping constant c describes the effects of viscosity for this macroscopic model and relates the force in the dashpot model to the speed of the piston in the viscous medium. It is related to, but is different from, the coefficient of viscosity η described in Chap. 7, which connects shear stress and the shear rate in a viscous fluid, as in (7.22) and (7.33).

We will combine these ideal springs and dashpots to arrive at models of realistic viscoelastic materials and see how they respond to stimuli that vary with time. We can examine the extensive properties of applied forces and deformations of the material or the corresponding intensive properties of stress and strain.

There are three interrelated manifestations of viscoelasticity (Fig. 4.44):

1. *Creep*. When a stress (or force) is applied and maintained, there is a strain (or deformation) in the medium that increases with time.

2. *Stress relaxation*. When a strain (or deformation) is applied and maintained, a stress (or force) is felt by the medium immediately, and it then relaxes in time.

3. *Hysteresis*. When stresses are applied and then released (forces loaded and unloaded), the stress–strain cycles are not reversible. Some, but not all, of the work done in the loading processes (during which the stress is increased) is recoverable in unloading (during which the stress is decreased).

Each of these effects can be observed and characterized by our models for *step function*, *impulse*, and *cyclic loading* (which are shown in the Fig. 4.45). There are also outcomes other than those predicted by our models—such as ordinary and stress fractures—from long-term static loading and many cycles of loading.

One feature of viscoelasticity is that materials behave differently over different time scales. This is seen for one well-known viscoelastic material, Silly Putty™. When you throw silly putty against a wall, it bounces back like a ball with Young's

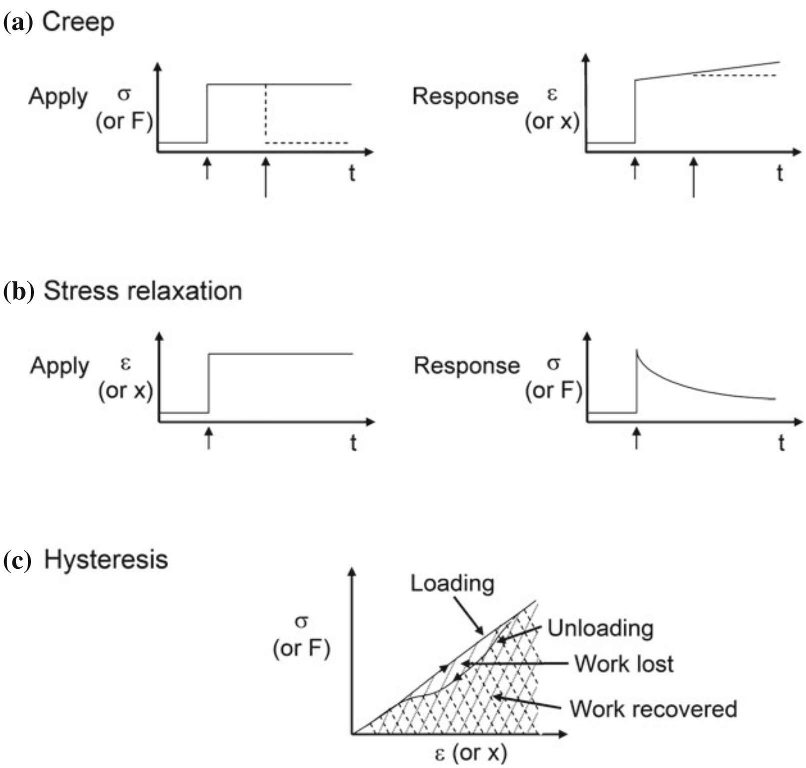

Fig. 4.44 General examples of **a** creep, **b** stress relaxation, and **c** hysteresis in viscoelastic systems. In (**a**) and (**b**) the stimulus is applied at the time of the *shorter arrow*. In (**a**) the possibility of removing the stimulus is also shown, at the time of the *longer arrow*, with the *dashed lines*. In (**c**) the recovered work is the area of the *cross-hatched region*, while the lost work is the area of the *lined region*. (More precisely, this is work per unit volume for stress σ and strain ϵ and work for force F and distortion x)

modulus $\sim 1.7 \times 10^6$ N/m^2 [15]. When you pull it, it stretches like putty with viscosity $\sim 8 \times 10^4$ Pa-s. In the first example it behaves elastically. The time scale, the collision time with the wall, is short, $\ll 0.1$ s. It behaves in a viscous manner in the second example, because the time scale of pulling on it is long, $\gg 0.1$ s.

Figure 4.46 shows the stress–strain curves for bone when it is strained at different strain rates. When bone is strained slower, it develops less stress for the same applied strain. Figure 4.47 shows when stress is applied at slower rates, there is more strain for the same applied stress. Hysteresis in bone is shown in Fig. 4.48. Hysteresis and stress relaxation are shown for ligaments, tendons, and passive muscles in Figs. 4.49 and 4.50. The mechanism and the response of stress relaxation for cartilage are depicted in Fig. 4.51. This involves the exudation of fluid from the cartilage, which is tied to the lubrication of synovial joints, as shown in Fig. 3.15. The elastic modulus

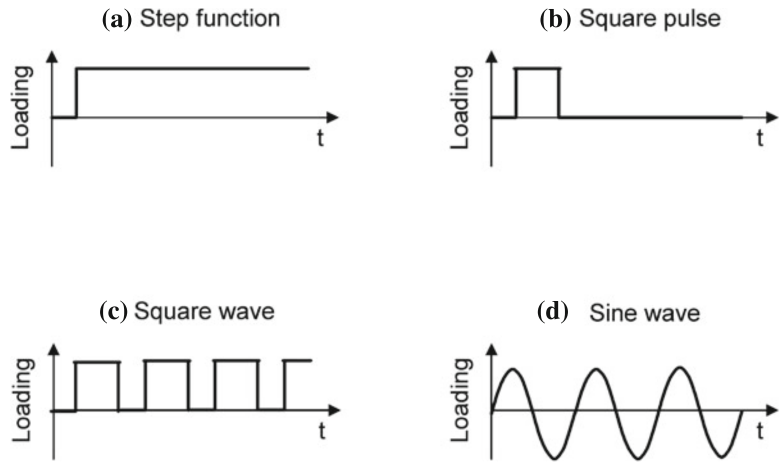

Fig. 4.45 Different types of loading protocols: **a** step function, **b** square pulse, and cyclic with **c** square pulses, or **d** sine waves

Fig. 4.46 Stress versus strain for cortical bone for different strain rates, showing increased modulus and strength with increased strain rate. (Based on [24, 45, 46])

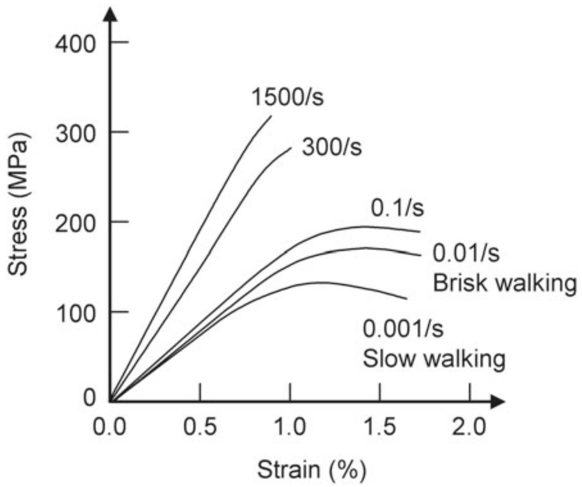

of cartilage increases from $\sim$1 MPa for very slow rates of loading to 500 MPa for fast rates. Some mechanical properties of cartilage are plotted for different strain rates in Figs. 4.52 and 4.53. The modulus is $\sim$0.70 MPa and Poisson's ratio = 0.10 for lateral femoral condyle cartilage.

Before developing models of viscoelastic materials, let us see how the perfect spring and dashpot components respond to idealized applications of stress and strain.

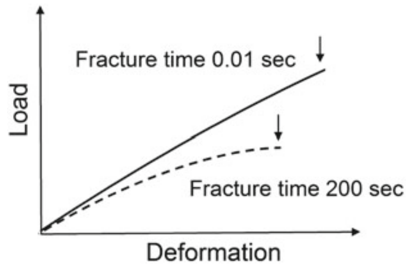

Fig. 4.47 Load (stress) versus deformation (strain) for dog tibiae for different loading rates. The *arrow* shows the point of failure. At higher loading rates the load and the energy to failure are almost doubled, where energy is the area under the curve. (Based on [12, 69])

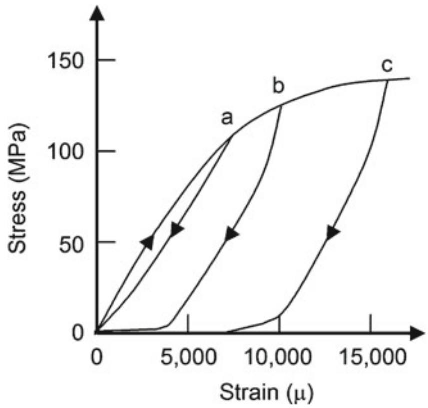

Fig. 4.48 Hysteresis in bone and shifting in the stress–strain curve with repeated loading (to a, b, c) and unloading. The units of strain are microstrain. (Based on [8, 18])

4.5.1 Perfect Spring

We use (4.47) to determine the response of a perfect spring to a stimulus. If we apply a force F_0 of any level, there will be an "instantaneous" deformation response of $x = F_0/k$. This creep response is seen in Fig. 4.54a for a step-like application of force. If we suddenly subject the material to a deformation x_0 (or a strain), with a step function ($\theta(t)$, as described below), there is an instantaneous step function response in the force (or stress) it feels (Fig. 4.54b).

4.5.2 Perfect Dashpot

Equation (4.48) describes the motion of a perfect dashpot with damping constant c. This characterization is often used to describe friction and other types of energy relaxation and dissipation. If we immediately apply a constant force F_0 at time $t = 0$,

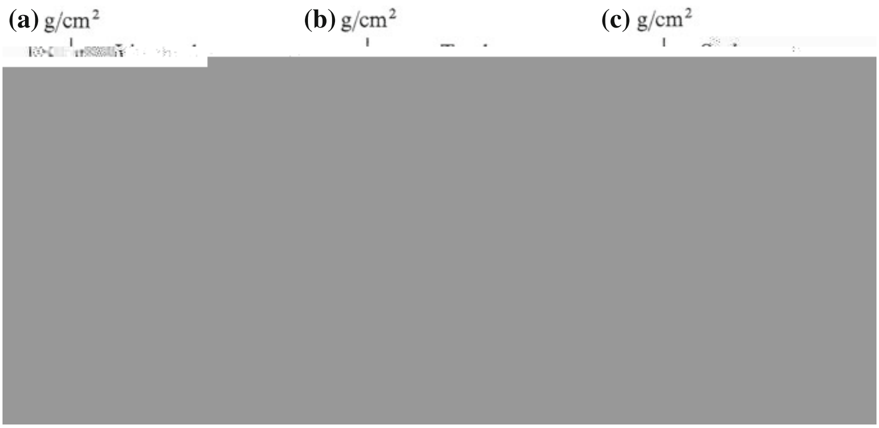

Fig. 4.49 Stress–strain hysteresis loop for nonvascular tissue: **a** the ligamentum nuchae (a ligament) (collagen denatured at 76° C, so it is mostly elastin), **b** tendon (mostly collagen), and **c** (passive) intestinal smooth muscle. The vertical axis units are those of stress when multiplied by g. (From [5, 25])

Fig. 4.50 Stress relaxation in nonvascular tissue: **a** the ligamentum nuchae (collagen denatured at 76° C, so it is mostly elastin), **b** tendon (mostly collagen), and **c** (passive) intestinal smooth muscle. The vertical axis units are those of stress when multiplied by g. (From [5, 25])

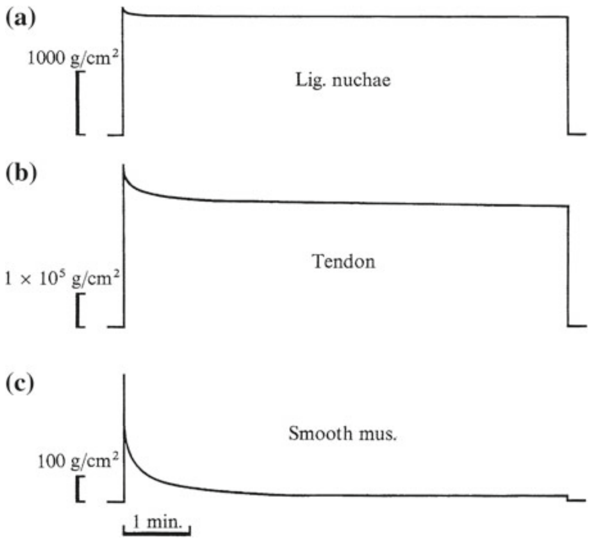

there is immediate motion with $v = \mathrm{d}x/\mathrm{d}t = F_0/c$. As seen in Fig. 4.55a, the dashpot piston is at position $(F_0/c)t$. This creep response stops suddenly when the force is removed, because $v = \mathrm{d}x/\mathrm{d}t$ immediately becomes zero. If we suddenly subject the material to a deformation x_0 (or a strain), with a step-like function, there is an immediate, very large, short-enduring force (described by a Dirac delta function response—see below) (Fig. 4.55b). With continued application of this deformation or strain, the force remains zero. Clearly, the responses of the dashpot and spring to applied stresses and applied strains are very different.

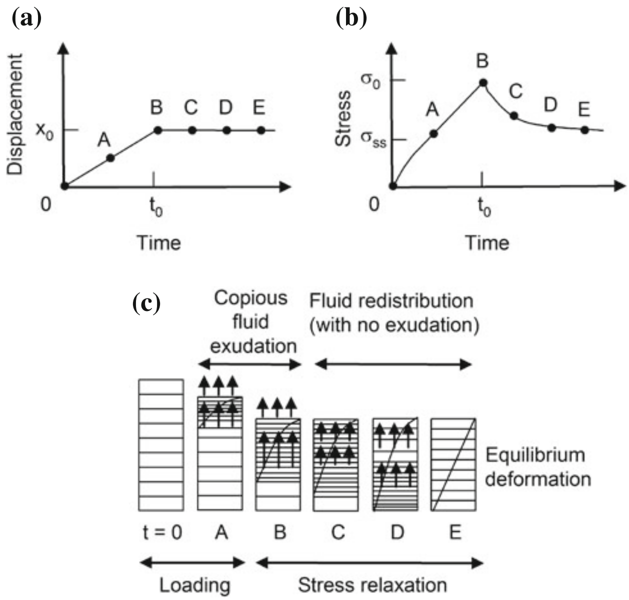

Fig. 4.51 **a** Controlled ramp deformation of cartilage from time 0 to t_0 and the **b** (viscoelastic) stress response, initially to σ_0, and later to the steady state value σ_{ss}, along with (**a**) and **c** physical model of the response. This response includes interstitial fluid flow (*arrows*)—initially out of and within the solid matrix and later only within the matrix—and also the deformation of the solid matrix of the cartilage. (Based on [32, 50, 52])

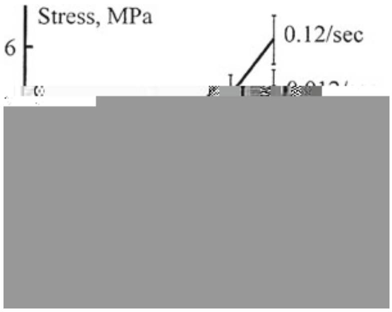

Fig. 4.52 Stress–strain for cartilage at different strain rates. (From [45], as from [73])

4.5.3 *Simple Viscoelastic Models*

Three models are commonly used to describe viscoelastic materials. Each combines these idealized springs and dashpots in different ways (see Fig. 4.56) [22, 27]. (a) A *Maxwell body* is a dashpot and spring in series. (b) A *Voigt body* is a dashpot and spring in parallel. (c) A *Kelvin body* is a dashpot and spring in series, which are in parallel with another spring. The Kelvin model is also called *the standard linear*

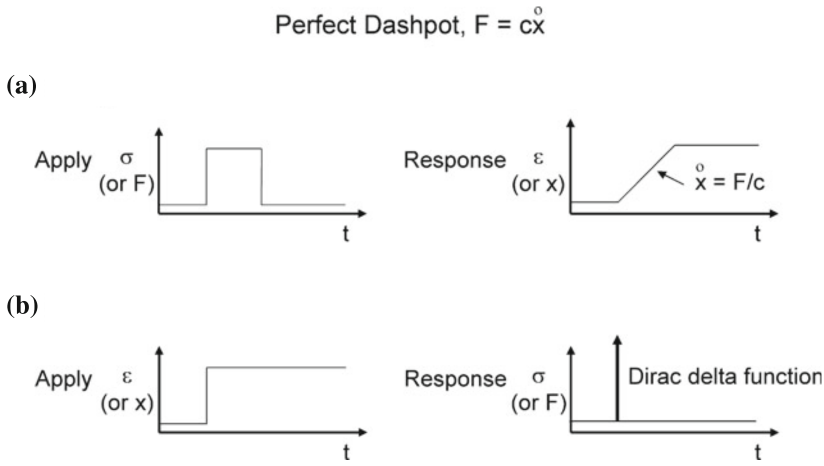

Fig. 4.55 Response by a perfect dashpot. **a** Creep. **b** Stress relaxation

$x_j^{\mathrm{T}} = x_j^{\mathrm{E}} + x_j$. Reference to an equilibrium length is important in describing springs, because $F = kx = k(x^{\mathrm{T}} - x^{\mathrm{E}})$.

Maxwell Model

The force F applied at the end of a Maxwell body (Fig. 4.56a) is felt equally by the dashpot (unit "1") and spring (unit "2"), so $F = F_1 = F_2$. Therefore, for the dashpot

$$F_1 = F = c\,\frac{\mathrm{d}x_1}{\mathrm{d}t}\left(= c\,\frac{\mathrm{d}x_1^{\mathrm{T}}}{\mathrm{d}t}\right) \tag{4.49}$$

and for the spring

$$F_2 = F = kx_2\ (= k(x_2^{\mathrm{T}} - x_2^{\mathrm{E}})). \tag{4.50}$$

The total length is $x^{\mathrm{T}} = x_1^{\mathrm{T}} + x_2^{\mathrm{T}}$, so $\mathrm{d}x^{\mathrm{T}}/\mathrm{d}t = \mathrm{d}x_1^{\mathrm{T}}/\mathrm{d}t + \mathrm{d}x_2^{\mathrm{T}}/\mathrm{d}t$. Because the equilibrium lengths do not vary with time ($\mathrm{d}x^{\mathrm{E}}/\mathrm{d}t = \mathrm{d}x_1^{\mathrm{E}}/\mathrm{d}t = \mathrm{d}x_2^{\mathrm{E}}/\mathrm{d}t = 0$), we find

$$\frac{\mathrm{d}x}{\mathrm{d}t} = \frac{\mathrm{d}x_1}{\mathrm{d}t} + \frac{\mathrm{d}x_2}{\mathrm{d}t}. \tag{4.51}$$

Using (4.49), we see that $\mathrm{d}x_1/\mathrm{d}t = F/c$. From (4.50), we see $x_2 = F/k$, and taking the first time derivative of both sides gives $\mathrm{d}x_2/\mathrm{d}t = (\mathrm{d}F/\mathrm{d}t)/k$. Using (4.51), we find

$$\frac{\mathrm{d}x}{\mathrm{d}t} = \frac{F}{c} + \frac{\mathrm{d}F/\mathrm{d}t}{k}. \tag{4.52}$$

This is the equation that relates the deformation $x(t)$ and force $F(t)$ for a Maxwell body. (Note how this reduces to the derivative of the relation for a perfect spring for large c and to the relation for a dashpot for large k.)

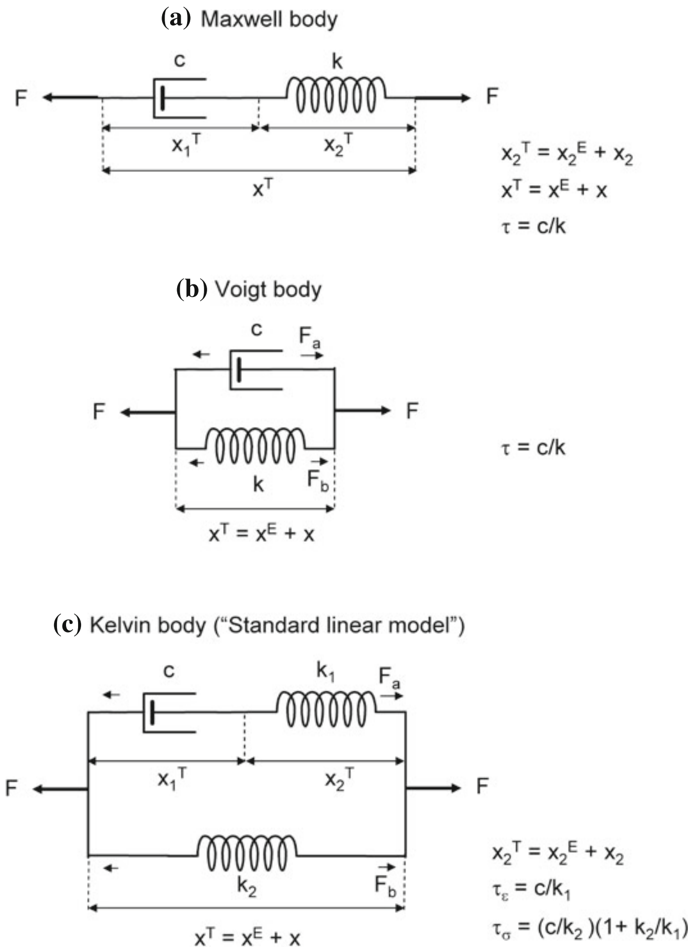

Fig. 4.56 Maxwell, Voigt, and Kelvin (standard linear model) mechanical models of viscoelasticity. The symbols for the springs and dashpots are the same as those used in Fig. 4.43. (Based on [25])

To test creep, a force F_0 is suddenly applied at $t = 0$. There is no change in the displacement of the dashpot, so $x_1^T = 0$ then. The spring immediately responds to give $x_2 = F_0/k$, so overall the initial condition is $x(0) = F(0)/k$ (for either creep or stress relaxation), and for $F(t = 0) = F_0$ it is $x(t = 0) = F_0/k$.

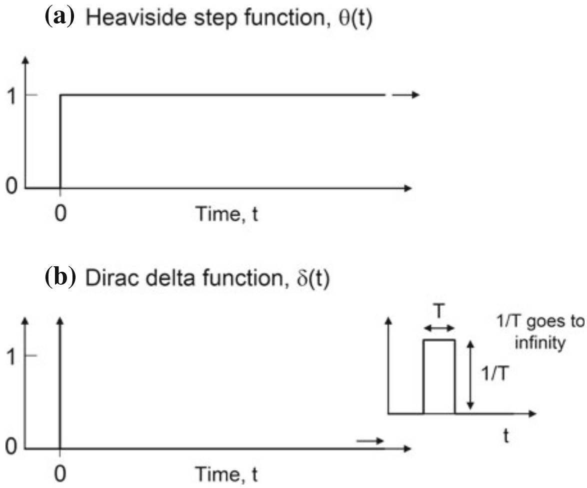

Fig. 4.57 **a** Heaviside step function $\theta(t)$ and **b** Dirac delta function $\delta(t)$. The area under the Dirac delta function remains 1, as the width $T \to 0$ and the height $1/T \to \infty$. If these functions start at a time other than $t = 0$, say at t_0, they are written as $\theta(t - t_0)$ and $\delta(t - t_0)$

The sudden application of a constant force F_0 can be represented by $F(t) = F_0\theta(t)$, where $\theta(t)$ is the Heaviside step function (Fig. 4.57a), alluded to earlier, which is

$$\theta(t) = 0 \text{ for } t < 0; \quad = 0.5 \text{ at } t = 0; \quad = 1 \text{ for } t > 0. \tag{4.53}$$

The time derivative $\mathrm{d}\theta(t)/\mathrm{d}t$ is the Dirac delta function $\delta(t)$ (Fig. 4.57b) which is zero for all t except at $t = 0$, when it approaches infinity in such a way that its integral over time remains unity, as in

$$\delta(t) = 0 \text{ for } t < -T/2; \quad = 1/T \text{ for } -T/2 < t < T/2; \quad = 0 \text{ for } t > T/2 \tag{4.54}$$

in the limit that T goes to 0. (Of course, the Heaviside step function is the integral of the Dirac delta function.)

To test stress relaxation, a deformation x_0 is suddenly applied at $t = 0$. There is no change in the force of the dashpot, so $F_1^{\mathrm{T}} = 0$ then. A sudden application of a constant deformation x_0 can be represented by $x(t) = x_0\theta(t)$.

The response of the Maxwell body to the applied force $F(t) = F_0\theta(t)$ is

$$x(t) = F_0\left(\frac{1}{k} + \frac{t}{c}\right)\theta(t) \tag{4.55}$$

and to the deformation $x(t) = x_0\theta(t)$ it is

$$F(t) = kx_0 \exp(-(k/c)t\theta(t)). \tag{4.56}$$

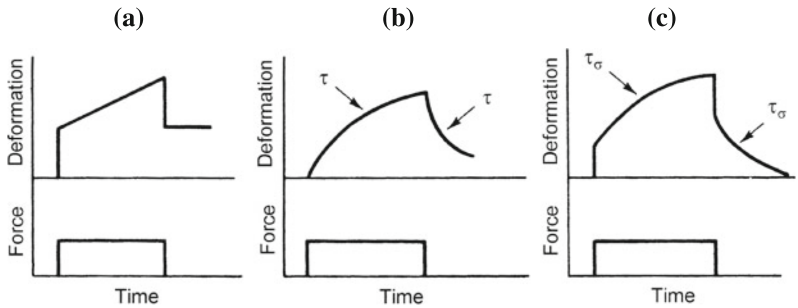

Fig. 4.58 Creep functions for the **a** Maxwell, **b** Voigt, and **c** Kelvin/linear standard models of viscoelasticity, with force loading and subsequent unloading. Characteristic relaxation times are shown. (From [25])

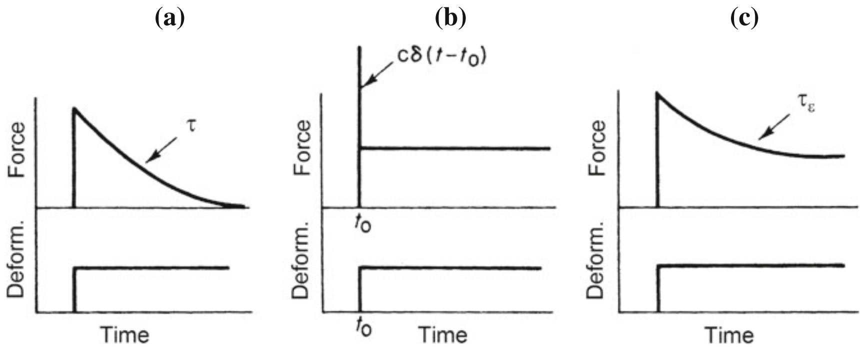

Fig. 4.59 Stress relaxation functions for the **a** Maxwell, **b** Voigt, and **c** Kelvin/linear standard models of viscoelasticity, with a step function deformation. Characteristic relaxation times are shown. (From [25])

These solutions can be proved by substitution in (4.52). (Also see Appendix C.) These results are plotted in Figs. 4.58a and 4.59a. (The plotted creep response is really that due to a sudden application of a constant force—say at time $t = 0$—and then suddenly turning it off—say at time $t = T$—and so the response to $F(t) = F(\theta(t) - \theta(t - T))$ is actually plotted for this and the other two models.)

In the creep experiment, there is an immediate spring-like response. Then the deformation increases (i.e., it creeps) linearly in time, as for the dashpot. When the force is removed, the deformation immediately decreases to the value determined by the spring component, and subsequently there is no more creep due to the dashpot. This is a simple linear combination of the responses seen for the individual elements in Figs. 4.54 and 4.55.

In the stress relaxation experiment, there is an immediate force response due to the spring element, but this response decreases in an exponential manner, as $\exp(-t/\tau)$, due to the dashpot. The parameter $\tau = c/k$ is called a time constant; it has the units of seconds. This response is clearly not a mere linear combination of the responses for the individual elements.

Voigt Model

The combination of the elements is simple (Fig. 4.56b). The total force is the sum of the individual forces on each element $F = F_1 + F_2$, and the deformations of both elements are equal and they are equal to the whole $x = x_1 = x_2$. Because $F_1 = c\ \mathrm{d}x_1/\mathrm{d}t = c\ \mathrm{d}x/\mathrm{d}t$ and $F_2 = kx_2 = kx$,

$$F = c\frac{\mathrm{d}x}{\mathrm{d}t} + kx. \tag{4.57}$$

The initial condition is $x(t = 0) = 0$ for any applied F, because the dashpot prevents any immediate deformation.

The response of the Voigt body to the applied force $F(t) = F_0\theta(t)$ is

$$x(t) = \frac{F_0}{k}(1 - \exp(-(k/c)t))\theta(t) \tag{4.58}$$

and to the deformation $x(t) = x_0\theta(t)$ it is

$$F(t) = cx_0\delta(t) + kx_0\theta(t). \tag{4.59}$$

Again, these solutions can be proved by substitution in (4.57). (Also see Appendix C.) These results are plotted in Figs. 4.58b and 4.59b.

In the creep experiments, there is an exponential increase in creep, as $1 - \exp(-t/\tau)$, due to the dashpot—where again $\tau = c/k$. If the force is removed, this deformation decays to zero exponentially as $\exp(-t/\tau)$. This is qualitatively different from the predictions of the Maxwell model.

In the stress relaxation experiments, there is an immediate and temporary Dirac delta function increase in force, as seen for the dashpot alone, and then the response is the constant value expected from the spring alone. Again, this is qualitatively different from the predictions of the Maxwell model.

Kelvin Model (The "Standard" Linear Model)

In this model (Fig. 4.56c) the spring constant of the spring in series with the dashpot is called k_1; it was called k in the Maxwell model. The spring constant in parallel with the dashpot and spring in series is called k_2; the analogous constant in the Voigt model was also called k.

The length of the dashpot is $x_1^{\mathrm{T}} = x_1^{\mathrm{E}} + x_1$, while that of the top spring is $x_2^{\mathrm{T}} = x_2^{\mathrm{E}} + x_2$. The total length

$$x^{\mathrm{T}} = x_1^{\mathrm{T}} + x_2^{\mathrm{T}} \tag{4.60}$$

is also the length of the bottom spring. As with the Maxwell body, the same force

$$F_{\mathrm{a}} = c\,\frac{\mathrm{d}x_1}{\mathrm{d}t} = k_1 x_2 \tag{4.61}$$

is felt across the top dashpot and spring; the force

$$F_{\mathrm{b}} = k_2 x \tag{4.62}$$

is felt across the bottom spring. As with the Voigt model, the total force across the parallel elements is

$$F = F_{\mathrm{a}} + F_{\mathrm{b}}. \tag{4.63}$$

Our goal is to derive an equation that has only F, $\mathrm{d}F/\mathrm{d}t$, x, and $\mathrm{d}x/\mathrm{d}t$. Using (4.61), we see $\mathrm{d}x_1/\mathrm{d}t = F_{\mathrm{a}}/c$ and $x_2 = F_{\mathrm{a}}/k_1$. The time derivative of the second expression gives $\mathrm{d}x_2/\mathrm{d}t = (\mathrm{d}F_{\mathrm{a}}/\mathrm{d}t)/k_1$. Because $\mathrm{d}x_i^{\mathrm{E}}/\mathrm{d}t = 0$, from the first time derivative of (4.60), we have

$$\frac{\mathrm{d}x}{\mathrm{d}t} = \frac{\mathrm{d}x_1}{\mathrm{d}t} + \frac{\mathrm{d}x_2}{\mathrm{d}t} = \frac{F_{\mathrm{a}}}{c} + \frac{\mathrm{d}F_{\mathrm{a}}/\mathrm{d}t}{k_1}. \tag{4.64}$$

Using (4.62) and (4.63), we find $F_{\mathrm{a}} = F - F_{\mathrm{b}} = F - k_2 x$. The first time derivative of this is $\mathrm{d}F_{\mathrm{a}}/\mathrm{d}t = \mathrm{d}F/\mathrm{d}t - k_2 \mathrm{d}x/\mathrm{d}t$. Using these in (4.64) gives

$$\frac{\mathrm{d}x}{\mathrm{d}t} = \frac{F - k_2 x}{c} + \frac{1}{k_1}\left(\frac{\mathrm{d}F}{\mathrm{d}t} - k_2\frac{\mathrm{d}x}{\mathrm{d}t}\right). \tag{4.65}$$

Collecting the force and deformation terms on opposite sides of the equation gives

$$F + \frac{c}{k_1}\frac{\mathrm{d}F}{\mathrm{d}t} = k_2 x + c\left(1 + \frac{k_2}{k_1}\right)\frac{\mathrm{d}x}{\mathrm{d}t}. \tag{4.66}$$

The second term on the left-hand side is absent in the Voigt model, while the first term on the right-hand side is absent in the Maxwell model. Factoring out k_2 gives

$$F + \frac{c}{k_1}\frac{\mathrm{d}F}{\mathrm{d}t} = k_2\left[x + \frac{c}{k_2}\left(1 + \frac{k_2}{k_1}\right)\frac{\mathrm{d}x}{\mathrm{d}t}\right]. \tag{4.67}$$

After introducing the time constants $\tau_\epsilon = c/k_1$ and $\tau_\sigma = (c/k_2)(1 + k_2/k_1) = c(1/k_1 + 1/k_2)$, this equation becomes

$$F + \tau_\epsilon\frac{\mathrm{d}F}{\mathrm{d}t} = k_2\left(x + \tau_\sigma\frac{\mathrm{d}x}{\mathrm{d}t}\right). \tag{4.68}$$

This tells us that the force terms relax with a time constant τ_ϵ, while the deformation terms relax with a time constant τ_σ. This is clear because the solution to $Q + \tau \, \mathrm{d}Q/\mathrm{d}t = 0$ is $Q(t) = Q(0)\exp(-t/\tau)$.

For a suddenly applied force or deformation, the initial condition is $\tau_\epsilon F(0) = k_2\tau_\sigma x(0)$. The response of the Kelvin body to the applied force $F(t) = F_0\theta(t)$ is

$$x(t) = \frac{F_0}{k_2}[1 - (1 - \frac{\tau_\epsilon}{\tau_\sigma})\exp(-t/\tau_\sigma)]\theta(t) \tag{4.69}$$

and to the deformation $x(t) = x_0\theta(t)$ it is

$$F(t) = k_2 x_0[1 - (1 - \frac{\tau_\sigma}{\tau_\epsilon})\exp(-t/\tau_\epsilon)]\theta(t). \tag{4.70}$$

Again, these solutions can be proved by substitution in (4.68). (Also see Appendix C.) These results are plotted in Figs. 4.58c and 4.59c.

In the creep experiments, there is an immediate increase due to the k_1 spring and then an exponential increase in creep, as $1 - \exp(-t/\tau_\sigma)$, due to the dashpot. When the force is removed, this strain decays to zero exponentially as $\exp(-t/\tau_\sigma)$.

In the stress relaxation experiments, there is an immediate finite increase in force, and then the response relaxes as $\exp(-t/\tau_\epsilon)$ to a constant value.

These predictions incorporate features from both the Maxwell and Voigt models. The Kelvin model also cures the clear deficiencies in them, such as the unphysical Dirac delta function in the stress relaxation response in the Voigt model.

4.6 Viscoelasticity in Bone

The stress in bone does not depend only on the current value of strain, but on how fast that strain was applied. Figure 4.46 shows that for a given strain the developed stress is larger when the strain is applied fast. Similarly, the strain in the bone depends not only on the current value of stress, but also on how fast that stress was applied. Figure 4.47 shows that for a given force load, the deformation is smaller when the load is applied fast.

We examine this second case quantitatively by using the Kelvin standard linear model. Let us apply a force F_0 in a linearly increasing manner over a time T. As seen in Fig. 4.60a, this means that $F = F_0(t/T)$ from $t = 0$ to $t = T$. We will determine the deformation $x(t)$, so we can obtain the deformation when the total force F_0 has been applied, $x(T)$ and see how $x(T)$ depends on T.

We use $F = F_0(t/T)$ and $\mathrm{d}F/\mathrm{d}t = F_0/T$ in (4.68) to get

$$k_2\left(x + \tau_\sigma\frac{\mathrm{d}x}{\mathrm{d}t}\right) = F + \tau_\epsilon\frac{\mathrm{d}F}{\mathrm{d}t} = F_0\frac{t}{T} + \tau_\epsilon\frac{F_0}{T} \tag{4.71}$$

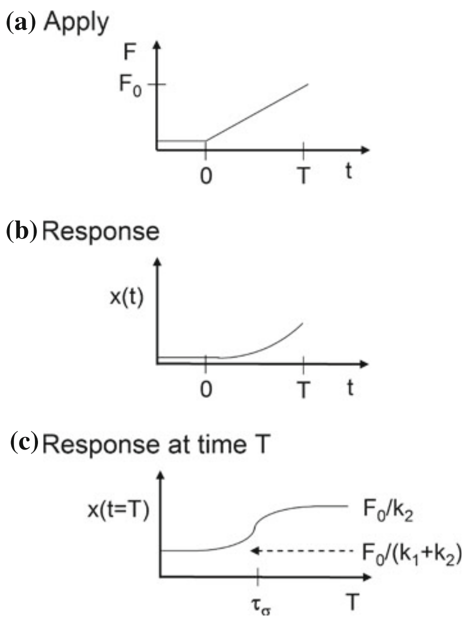

Fig. 4.60 The deformation (in (**b**)) resulting from a linearly increasing applied force (in (**a**)). The deformation from (**b**) at the end of the ramp, $t = T$, is plotted in (**c**) as a function of the ramp time T, which is referenced to τ_σ

or

$$x + \tau_\sigma \frac{\mathrm{d}x}{\mathrm{d}t} = \frac{F_0}{k_2 T} t + \frac{\tau_\epsilon F_0}{k_2 T}, \tag{4.72}$$

with $x(t = 0) = 0$.

This equation has the form

$$x + a \frac{\mathrm{d}x}{\mathrm{d}t} = bt + e, \tag{4.73}$$

which has a solution

$$x(t) = bt + (e - ab)(1 - \exp(-t/a)), \tag{4.74}$$

that satisfies $x(t = 0) = 0$. The form of this solution can be verified by inserting it into the original equation. Such a substitution also gives a, b, and e, which leads to the final solution

$$x(t) = \frac{F_0}{k_2 T} t - \frac{c F_0}{k_2^2 T}(1 - \exp(-t/\tau_\sigma)). \tag{4.75}$$

(See Appendix C.) Clearly, this is valid only for $0 < t < T$. This solution can be checked in Problem 4.35, and is plotted in Fig. 4.60b. For $t \ll \tau_\sigma$, $x(t) \approx F_0(t/T)/(k_1 + k_2)$.

The deformation $x(T)$ at the end of the force ramp is

$$x(t = T) = \frac{F_0}{k_2} - \frac{cF_0}{k_2^2 T}(1 - \exp(-T/\tau_\sigma)), \tag{4.76}$$

which is plotted in Fig. 4.60c as a function of T. Applying the force quickly or slowly really means that the time T is either much shorter or longer than the time constant, τ_σ. In these limits:

$$x(T) \to \frac{F_0}{k_1 + k_2} \text{ when } T \ll \tau_\sigma \text{ and } \to \frac{F_0}{k_2} \text{ when } T \gg \tau_\sigma. \tag{4.77}$$

This model agrees with the experimental observations that the deformation is less with faster loading (Fig. 4.47 for bone). More generally, the terms "fast" and "slow" are relative to a characteristic time constant, which in this case is τ_σ. The analogous stress relaxation experiment can be modeled in a similar way with the relevant time constant τ_ϵ, and is addressed in Problem 4.38.

4.7 Bone Fractures

Bones in the skeleton are designed for several properties and functions. Muscles create motion by swinging bones at articulations. With relatively stiff bones, the muscles can be efficient in that when they contract they do not cause the bones to deform. Stiff bones absorb relatively little energy before they fracture (see below), whereas more compliant bones resist fracture more and are lighter (and there is less mass for the body to lug around)—but they are less ideal for muscle action. Nature compromises as needed. In children, efficiency of motion is less important than resistance to fracture. The femoral bone is about 2/3 as stiff in children as in adults and requires about 50% more energy to break. The bones of the inner ear need to be stiff to transmit sound waves efficiently, but do not need to resist fracture because they bear no loads.

We now consider the *work of fracture* W_F, which is the amount of work that has to be performed on a material to break it. It is usually defined as the energy (J) needed for fracture per area (m^2). This can be estimated from the elastic energy stored using the stress–strain curves earlier in this chapter. Materials that have a higher work of fracture are *tougher* than those with a lower one (Fig. 4.16). Typical values are 1–10 J/m^2 for glass, $\sim$1,000 J/m^2 for nylon, $\sim$10,000 J/m^2 for wood, and 10^3–10^4 J/m^2 for bone. Materials with the same strength (UTS) are tougher (i.e., they require more energy to fracture) when they are less stiff (smaller Y), because the elastic energy stored per unit volume is $\mathrm{PE}/V = \sigma^2/2Y = (\mathrm{UTS})^2/2Y$ (4.17) in the linear stress–strain limit.

Table 4.5 shows that the mechanical properties of typical femurs, deer antlers, and tympanic bulla (which are bony capsule housings in the ear) are quite different, even

Table 4.5 Physical properties of different types of bone

Property	Femur	Antler	Bulla
Young's modulus (Y) (GPa)	13.5	7.4	31.3
Ultimate bending stress (UBS) (GPa)	247	179	33
Work of fracture (W_F) (J/m^2)	1,710	6,190	200
Density (g/cm^3)	2.06	1.86	2.47

From [47]. Using data from [16]

though they have comparable densities. Femurs support weight during movement and need to be stiff (large Y), strong (large *ultimate bending stress*, UBS—see below), and tough (large W_F). Deer antlers need to be very tough with a very high work of fracture to avoid breakage in deer fights (and they are tougher than femurs), but they do not need to be really stiff or strong. Tympanic bulla house the middle/inner ear and keep out sounds other than those coming through the ear canal. This helps directional hearing, with sounds detected in each ear at different times. This acoustic separation is improved by increasing the ratio of Y for the bulla and water (see Chap. 10); Y for bulla is very high. The bulla do not need to be strong or tough. If forces were applied that would be large enough to break them, the person would be dead anyway.

4.7.1 Modes of Sudden Breaking of Bones

Let us revisit the example from earlier in this chapter, when we considered how much the femur shortens at the UCS $= 170\,\text{MPa} = 170\,\text{N/mm}^2$. With no stress applied, the femur is $L_0 = 0.5\,\text{m} = 500\,\text{mm}$ long and has a cross-sectional area $A = 370\,\text{mm}^2$. The UCS is reached when there is a force of $(170\,\text{N/mm}^2)(370\,\text{mm}^2) = 56,000$ N $= 12,600\,\text{lb} \sim 6$ tons on the femur. For a 70 kg person (700 N, 160 lb), this is 80× body weight. Because the maximum force on the hip bone and femur during walking is ∼2× body weight and during running it is ∼4× body weight, we are fortunately well designed. There is a much larger overdesign protection in the long leg bones during running than in the Achilles tendon!

The potential energy available during a fall to the ground from standing is $m_b g(\Delta h_{CM})$. A 1.8 m tall person of mass 70 kg, has a center of mass 0.9 m above the ground. When this person falls, the center of mass decreases to 0.1 m and the available potential energy is $m_b g(\Delta h_{CM}) = (70\,\text{kg})(9.8\,\text{m/s}^2)(0.8\,\text{m}) \approx 550\,\text{J}$.

How much energy is stored in the bones during this fall? Let us examine the largest bone, the femur. We use (4.17) with $L_0 = 0.5\,\text{m} = 500\,\text{mm}$ and $A = 330\,\text{mm}^2$, and so $V = 165{,}000\,\text{mm}^3$, and $Y = 17{,}900\,\text{MPa} = 17{,}900\,\text{N/mm}^2$. If the stress is either the UTS $= 122\,\text{MPa} = 122\,\text{N/mm}^2$ or UBS (ultimate bending stress, as described below) $= 170\,\text{MPa} = 170\,\text{N/mm}^2$ (Table 4.6), then respectively in the harmonic limit

Table 4.6 Properties of long bones

Bone	Y ($\times 10^4$ MPa)	UTS ($\times 10^2$ MPa)	UBS ($\times 10^2$ MPa)
Femur	1.72	1.21	2.08
Tibia	1.80	1.40	2.13
Fibula	1.85	1.46	2.16
Humerus	1.71	1.22	2.11
Radius	1.85	1.49	–
Ulna	1.84	1.48	–

From [6]. Using data from [79]

$$\mathrm{PE} = \frac{(\mathrm{UTS})^2}{2Y} V = \frac{(122\,\mathrm{N/mm^2})^2}{2 \times 17{,}900\,\mathrm{N/mm^2}}\, 165{,}000\,\mathrm{mm^3} \simeq 69\,\mathrm{J} \tag{4.78}$$

$$= \frac{(\mathrm{UBS})^2}{2Y} V = \frac{(170\,\mathrm{N/mm^2})^2}{2 \times 17{,}900\,\mathrm{N/mm^2}}\, 165{,}000\,\mathrm{mm^3} \simeq 133\,\mathrm{J}. \tag{4.79}$$

The energy needed to break long bones is clearly a reasonable fraction of that available from the kinetic energy in common collisions, such as falls. If the available energy is distributed to several of the long bones, there is enough for sudden fracture. Our bones do not regularly break because most of the energy is absorbed by muscle contractions and the deformation of soft tissues. Loads normal to skin, fat, and muscles (and clothing) absorb energy upon compression and propagate stress waves in the body. Fascia, tendons, ligaments, joint capsules, and contracted muscles brace bones against bending by supporting part of the tensile forces and absorbing energy as they are stretched. In elderly people bones fracture more easily because their bones are weaker (because they are more porous, Fig. 4.19), their tissues are less suited to absorb energy, which causes even more energy to be transmitted to the (already weaker) bones, and they may fall more awkwardly and with less body breaking action.

Bone fractures are determined by the mode of the applied loads and their orientations. Bones are strongest in compression, less strong in tension, and weakest in shear. Under some loading conditions there are tensile and shear or compressive and tensile loads at a given position. Bones usually break by shear (twisting) stresses or under tension, but not under compression because UTS $<$ UCS. Figure 4.61 shows crack formation in bent and twisted long bones. Under bending there is tension on one side and compression on the other. Because UTS $<$ UCS, the fracture starts at the side with tension. There are shear stresses at 45° to this load axis, but the tensile stress is larger on the left side, so the crack propagates normal to the bone axis. On the compressed side the shear stress (at 45°) is large and the compressive stress is $<$UCS, so cracking occurs at two 45° angles, leading to the *butterfly fragment* seen in the figure. In twisting, the tensile stresses produce a spiral crack that winds around the bone and the bone breaks when the ends of the crack are connected by a longitudinal fissure [45].

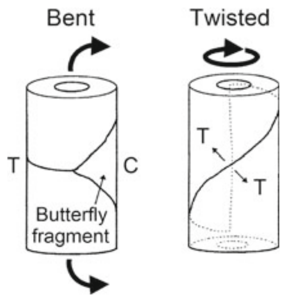

Fig. 4.61 Crack propagation in bent and twisted bone. T means tension and C means compression. (From [45])

Fracture can be due to direct blows, such as by blows to the soft tissue surrounding the bone or by bullets, which break the bone in two (*noncomminuted*) at low energy—leading to a *transverse* fracture, or into many pieces (*comminuted*) at high energy (Fig. 4.62) [3, 40, 54]. Indirect blows, as in skiing, can lead to fractures that are *spiral*, *oblique*, transverse with a butterfly fragment, and so on (Fig. 4.62). The nightstick fracture of the ulna, shown in Fig. 4.63, is one type of low-energy, direct-blow injury, and it is transverse. Figure 4.64 depicts the classification of humerus fractures. (Analogous classifications exist for other bones as well.)

As with any collision, we can lessen the likelihood of bone breakage in falls by increasing the impact area and the collision time. Because bones are actually viscoelastic, they absorb shocks a bit, which lessens the chance of fracture.

Breaking of Bones by Bending

Let us say we have a bone of thickness d that is symmetrical in the y direction. *Will it break when bent by a force F like the one in Fig. 4.31?*

We use the analysis we developed earlier this chapter. Equation (4.36) tells us that $\sigma(y) = Y(y/R)$, so with $y = d/2$ on the top surface and $-d/2$ on the bottom, the maximum compressive and tensile stresses have magnitudes (Fig. 4.34)

$$|\sigma_{\text{max,compression}}| = |\sigma_{\text{max,tension}}| = Y\frac{d}{2R}. \tag{4.80}$$

We would expect that the bone will break if either $|\sigma_{\text{max,compression}}| > \text{UCS}$ or $|\sigma_{\text{max,tension}}| > \text{UTS}$. Because UCS $= 170\,\text{MPa}$ and UTS $= 120\,\text{MPa}$, we would expect that the fracture will occur first in tension and consequently on the bottom surface for hard bone (Fig. 4.35). However, this fracture really occurs at a slightly higher value called the *ultimate bending stress* (UBS). The UBS is higher than UTS for the long bones, as in seen in Table 4.6. This table also shows that the mechanical properties of the long bones in the leg and arm are very similar, but not identical.

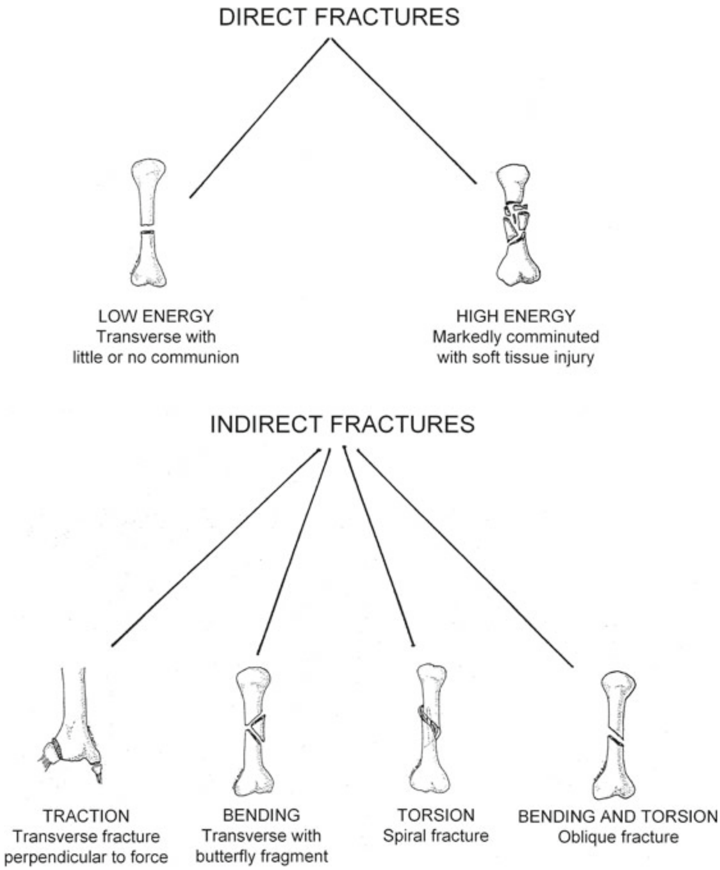

Fig. 4.62 Types of bone fractures resulting from different types of loading. (From [40])

Fig. 4.63 X-ray of a nightstick fracture of the ulna bone. (From [40])

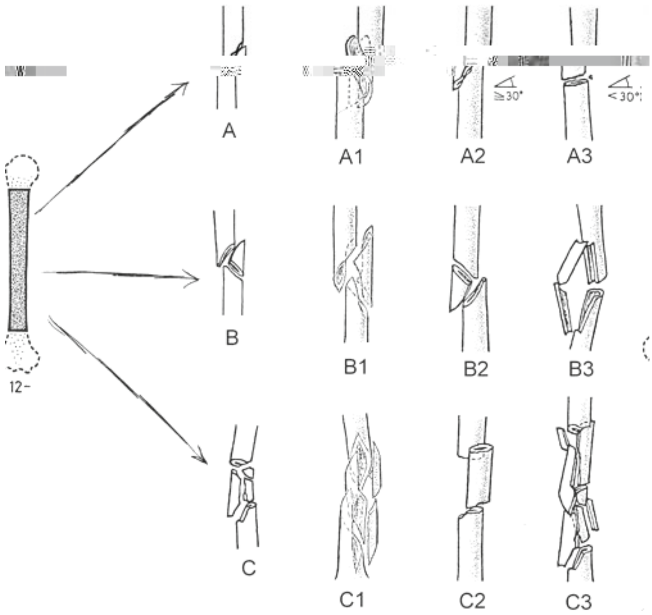

Fig. 4.64 AO-ASIF classification of humerus diaphysis fractures. *A* Simple fractures; *A1* spiral, *A2* oblique (≥30°), *A3* transverse (<30°); *B* wedge fractures; *B1* spiral wedge, *B2* bending wedge, *B3* fragmented wedge; *C* complex fractures; *C1* spiral, *C2* segmental, *C3* irregular. (From [40])

Fracture occurs when

$$|\sigma_{\mathrm{max,bending}}| > Y\frac{d}{2R_{\mathrm{min}}} = \mathrm{UBS}. \tag{4.81}$$

Using (4.40) for the curvature, $1/|R| = |M_\mathrm{B}|/YI_\mathrm{A}$, the bone breaks for bending moments

$$|M_\mathrm{B}| \geq \frac{2(\mathrm{UBS})I_\mathrm{A}}{d}. \tag{4.82}$$

Let us consider the example of one foot pinned at the ankle, while the other foot is slipping [6]. The pinned foot could be in a hole in frozen snow, pinned during a football tackle, or in a rigid ski boot. This situation is modeled in Fig. 4.65, where we see the force of the body (minus that of the leg) $W_\mathrm{b} - W_\mathrm{leg}$, creates a torque about the leg with a moment arm D of magnitude $D(W_\mathrm{b} - W_\mathrm{leg})$. D is the lateral distance of the midline of the body (center of mass) from the pinned leg, and so

$$|M_\mathrm{B}| = D(W_\mathrm{b} - W_\mathrm{leg}) \geq \frac{2(\mathrm{UBS})I_\mathrm{A}}{d}. \tag{4.83}$$

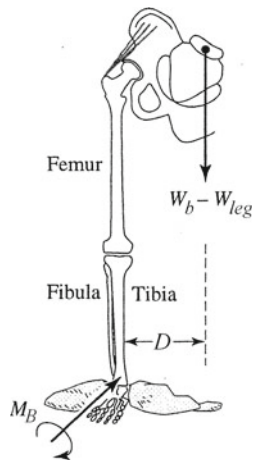

Fig. 4.65 Illustration of the origin of the bending moment in a person with a pinned ankle, as during falling. (From [6])

If the bone has a radius a, then $I_A = \pi a^4/4$ (because we can ignore the hollow nature of the bone in this estimate) and using $d \sim 2a$, the bone breaks when the moment arm

$$D \geq \frac{\pi a^3}{4} \frac{\text{UBS}}{W_b - W_{leg}}. \tag{4.84}$$

The tibia has its smallest cross-section about 1/3 of the way up from the ankle, where $a \sim 1$ cm. It is much thinner there than the humerus anywhere. The fibula is even narrower, but bears much less of the force than the tibia. For $W_b - W_{leg} = 640$ N (145 lb) (for a 75 kg, 750 N, 170 lb person), this shows that fracture occurs when the midline of the body moves more than 25 cm from the pinned leg during the slip.

This approach is also valid for the fast collisions encountered in the rapid hand and foot strikes used in karate. See the discussion in Chap. 3 about using this approach to analyze the breaking of boards in demonstrations of karate.

Euler Buckling (Advanced Topic)

The occurrence of fractures depends on the ultimate strength, defects, and specifically how loads are applied. Another type of macroscopic failure is buckling. This *Euler buckling* can be demonstrated by pushing down on a drinking straw that is standing upright on a table. When long thin tubes are compressed, the middle bows to one side and collapses. This mode of failure is associated with the stiffness of the material, and not its strength. This is different from the bending that occurs when a bar along the x-axis is fixed at one end, and the free end is pushed by a force F in the y direction (normal to the x-axis), as with bending in (4.44)–(4.46) and Fig. 4.40; the moment there is the force along the y-axis $\times$ the moment arm along x. Here the force is actually applied along the y-axis.

Let us consider a bar or column of length L fixed at both ends ($x = 0$ and $x = L$) with a compressive load S applied along the x-axis (Fig. 4.66a). The moment M_B in (4.44) now becomes Sy because the y-axis is normal to the applied force, so the curvature, from (4.40) and (4.44), becomes

$$\frac{d^2y}{dx^2} = -\frac{Sy}{YI_A}, \tag{4.85}$$

where Y is Young's modulus and I_A is the area moment of inertia. So we see that

$$\frac{d^2y}{dx^2} + \lambda^2 y = 0, \tag{4.86}$$

where we have used $\lambda^2 = S/YI_A$. This has a solution

$$y(x) = A \sin \lambda x + B \cos \lambda x, \tag{4.87}$$

which can be proved by substituting this into the previous equation (see Appendix C). The constant $B = 0$ because $y = 0$ at $x = 0$ and so $y(x) = A \sin \lambda x$. Because $y = 0$ at $x = L$, either $A = 0$ or $\sin \lambda L = 0$. The former boundary condition implies the bar will always be straight, while the latter allows for the possibility of buckling (with indeterminate and conceivably very large amplitude A). This latter condition is satisfied by $\lambda L = n\pi$, with $n = 1, 2, 3, \ldots$. This means $\lambda^2 = S/YI_A = n^2\pi^2/L^2$, so $S = n^2\pi^2 YI_A/L^2$. The lowest load that this buckling can occur at is the critical load S_c with $n = 1$

$$S_c = \frac{\pi^2 YI_A}{L^2}. \tag{4.88}$$

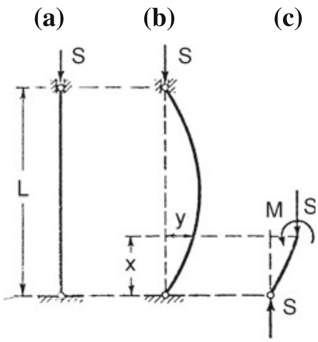

Fig. 4.66 **a** Before and **b** after Euler buckling of a bar or column. The bottom of the bar corresponds to $x = 0$ and $y = 0$. **c** A free body diagram of a part of the bar showing the external and internal forces and the moments acting on this column. (From [26])

For a beam of radius a and thin wall of thickness $w \ll a$ ($a_2 = a, a_1 = a - w$), $I_{\mathrm{A,hollow}} = \pi a^3 w$, so $S_\mathrm{c} = \pi^3 Y a^3 w / L^2$. Consequently, although making the walls of bone progressively thinner does not hurt its resistance to bending per unit mass, it will buckle more easily.

4.7.2 Stress Fractures (Advanced Topic)

We have seen that bones can fracture when the stress on them suddenly exceeds a given failure limit. They can also fracture more gradually from damage from prolonged continuous stress (creep, as with sitting) or prolonged *cyclic* stress (*fatigue*, as with walking or running) (Fig. 4.67). When the rate of damage exceeds the rate of repair by the body (known as *remodeling*), the bone fails as a result of a *stress fracture*.

We will now assess the occurrence of such fractures by looking at the applied stress and the resulting strains. From earlier in this chapter, we know that the microstrain in long bones is ∼10,000 $\mu\epsilon$ (1%) at the UCS. This is usually not reached. The peak functional microstrain in bones in most animals is between 2,000 and 3,000 $\mu\epsilon$ at peak performance. Strains in thoroughbred horses are routinely 5,000–6,000 $\mu\epsilon$ during racing. In humans, some studies indicate that the peak functional microstrains in the tibia, where stress fractures often occur, do not exceed 2,000 $\mu\epsilon$, while others

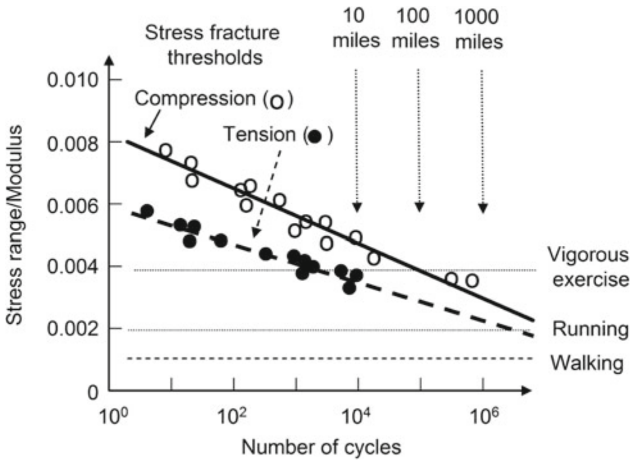

Fig. 4.67 Test strain ranges in compression and tension that lead to fatigue damage (stress fractures) in human cortical bone when applied for given number of cycles, referenced to the strains that simulate walking, running, and other strenuous exercise. There are approximately 5,000 cycles of testing (each corresponding to a step) in 10 miles (16 km) of running (which are the ranges of strain in either compressive or tensile loading experiments that simulate walking, running, and other strenuous exercise). (Based on [11, 24])

suggest that microstrains over 3,000 $\mu\epsilon$ can occur during jumping; this explains why "shin splints" are not uncommon among basketball players.

The study of how a flaw or crack grows under stress and leads to catastrophic failure is called *fracture mechanics*. The derivation of relations of linear elastic fracture mechanics is beyond the level of this text (see [45, 49, 62, 70]). Nonetheless, we will present some results from this field to help us understand stress fractures better.

Let us consider a thin plate with an elliptical hole with minor and major radii a and b, as in Fig. 4.68. With stress s applied parallel to the minor axis, the stress is maximum at the semimajor axis end as shown, and has magnitude

$$\sigma = s\left(1 + \frac{2a}{b}\right). \tag{4.89}$$

(The value of stress far from the crack is the applied stress s.) As a becomes much greater than b, the ellipse becomes narrower and begins to look more like a crack; then this relation is no longer valid. The stress pattern can then be determined, and expressed as a function of the distance from this same point (the end of the major axis) r and the angle from this axis θ, as shown in Fig. 4.68. For a given r, the stress is a maximum for $\theta = 0°$ (which makes sense from symmetry) and it varies as

$$\sigma = s\sqrt{\frac{a}{2r}}. \tag{4.90}$$

The stress increases nearer and nearer the crack (as r becomes small), but it does not really become infinite at the crack as this expression would suggest. The distance dependence can be brought to the left-hand side to obtain the stress intensity $\sigma(2r)^{1/2} = sa^{1/2}$. A stress intensity factor K is commonly defined, which is fairly similar to this stress intensity with the same (stress)(distance)$^{1/2}$ units, but it is more general:

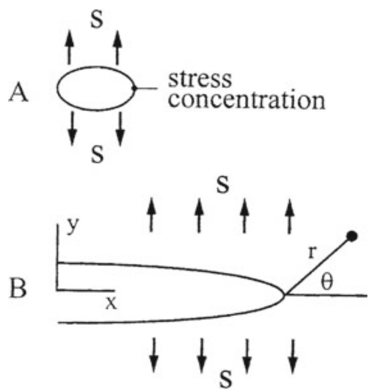

Fig. 4.68 An elliptical hole in a plate structure with stress tension s has much higher stress at the concentration point shown. (From [45])

Table 4.7 Fracture toughness of materials

Material	K_c (MPa-m$^{1/2}$)
2024 aluminum	20–40
4330V steel	86–110
Ti–6Al–4V	106–123
Concrete	0.23–1.43
Al_2O_3 ceramic	3.0–5.3
SiC ceramic	3.4
PMMA polymer	0.8–1.75
Polycarbonate polymer	2.75–3.3
Cortical bone	2.2–6.3

From [45]

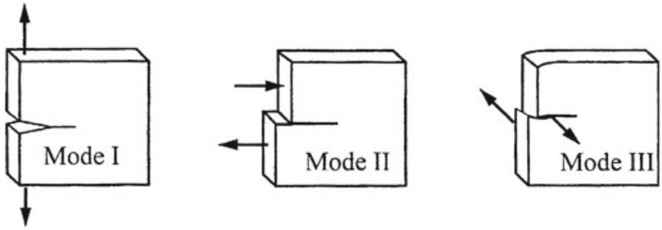

Fig. 4.69 Modes of cracking: I, the opening mode; II, the forward shear or sliding mode; III, the antiplane shear or tearing mode. (From [45])

$$K = Cs\sqrt{\pi a}. \tag{4.91}$$

C is a dimensionless constant that depends on the size and shape of the crack and object, and how the stress is loaded. If K exceeds a critical value, the fracture toughness K_c, the crack will propagate; the larger K is above this value, the faster the crack will propagate. If it is smaller, it will not propagate. K_c is an intensive property of the material (Table 4.7).

Figure 4.69 shows three ways stresses can be applied to cause crack propagation, to the right in each picture. In Mode I the load is tensile (and here vertical) and perpendicular to the crack propagation direction, as in splitting a log lengthwise. In Mode II the load is shear, and parallel to the plane of the crack and the direction of crack propagation. In Mode III the shear load is perpendicular to the crack direction, as in tearing paper.

For Mode I cracks the constant C in (4.91) differs for different crack locations, such as those shown in Fig. 4.70. For a plate of width w under tension and a crack of length a on one edge, this constant is

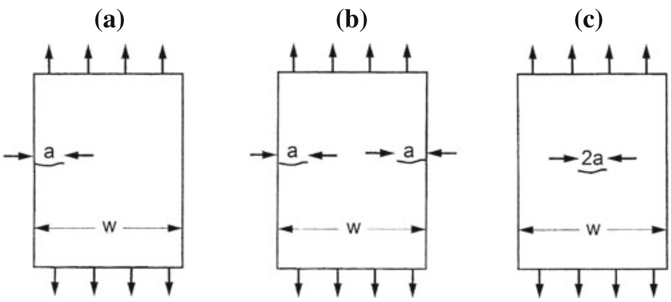

Fig. 4.70 Types of fracture for Mode I cracks, with **a**–**c** corresponding to (4.92)–(4.94), respectively. (Adapted from [45])

$$C = \frac{0.752 + 2.02q/\pi + 0.37(1 - \sin(q/2))^3}{\cos(q/2)} \sqrt{\frac{2}{q} \tan(q/2)} \tag{4.92}$$

using $q = \pi a/w$.

For cracks of length a on both edges, it is

$$C = (1 + 0.122 \cos^4(q))\sqrt{\frac{1}{q} \tan(q)}. \tag{4.93}$$

For a crack of length $2a$ in the center, it is

$$C = \left(1 - 0.10 \left(\frac{q}{\pi}\right)^2 + 0.96 \left(\frac{q}{\pi}\right)^4\right) \sqrt{\sec(q)}. \tag{4.94}$$

For cortical bone, $K_c = 2.2$–$5.7\,\text{MPa-m}^{1/2}$ for a Mode I transverse fracture of the tibia and a Mode I longitudinal fracture of the femur. It is 2.2–$2.7\,\text{MPa-m}^{1/2}$ for a Mode II fracture of the tibia. In each case the crack propagation is parallel to the long axis of the bone. Transverse propagation of cracks in long bones, perpendicular to the lamellar structure, causes the crack to turn along the long axis. Crack propagation in long bones is very anisotropic. The laminate structure of bones can stop or redirect a crack.

For a small crack in a large plate $q = \pi a/w \ll 1$, for which (4.92)–(4.94) each gives $C \sim 1$, and the critical condition is $K = K_c \sim s(\pi a_c)^{1/2}$ or

$$a_c \sim \frac{K_c^2}{\pi s^2}. \tag{4.95}$$

As before, if the body weight of 700 N (for a 70 kg person) were distributed over the femur cross-sectional area $370\,\text{mm}^2$, the stress $s = 2.1\,\text{N/mm}^2$. Because $1\,\text{MPa} = 1\,\text{N/mm}^2$, a typical $K_c = 4\,\text{MPa} - \text{m}^{1/2} = 4\,\text{N/mm}^2\text{–m}^{1/2}$. This gives $a_c \sim 1\,\text{m}$.

Does it make sense that a crack in the femur would have to be 1 m long for the bone to spontaneously fracture—especially when we know the bone is shorter and much narrower than this? Yes, because we would expect (and hope) that normal people would not get stress fractures by standing on one leg. If a_c were very small $\sim$1 mm, then our bones would fracture with the slightest of flaws when we stood up. If the stress were $10\times$ larger (corresponding to $10\times$ body weight), the critical crack length would be $100\times$ shorter or $\sim$1 cm. Also, note that our initial $a_c \sim 1$ m result violates the $q = \pi a/w \ll 1$ assumption we made that led to $C \sim 1$. We could have used the exact form(s) for C, but still would have obtained a large value for a_c.

The energy needed to break bonds in cracking comes from stored elastic energy. Cracks grow when the decrease in strain energy (from strain relief) $\mathrm{d}U/\mathrm{d}a$ ($= G$, *the strain energy release rate*) that occurs from the crack propagating a distance a exceeds or equals the energy or work $\mathrm{d}W$ needed to propagate the crack a distance a, which is $\mathrm{d}W/\mathrm{d}a$ (= *crack growth resistance* R). The strain energy release rate for Mode I cracks is [45]

$$G = \frac{\mathrm{d}U}{\mathrm{d}a} = \frac{\pi a s^2}{Y}. \tag{4.96}$$

for a crack of length a and stress s. Using (4.91),

$$G = \frac{K^2}{CY}. \tag{4.97}$$

There is much more understood about fracture, which we will not cover [31, 45, 70]. For example, the elastic model presented here ignores the plastic deformation that occurs very near the crack.

4.8 Common Sports Injuries

As we have seen, damage to bones, ligaments, muscles, etc. can result from collisions, excessive stress or strain, and from repeated use with moderately large stresses. These often lead to injuries in sports, including injuries to the following [36, 48]:

Head

1. *Concussions* are described in Chap. 3, and are common in boxing, football, and hockey. They also occur in baseball when pitchers successfully throw at batters' heads.

Shoulder

1. In a *separated shoulder* there is ligament damage that can occur from collisions in several sports. Ligament stretching is a first degree separation, a slight tear is a second degree injury, and a complete tear is a third degree injury.

2. In a *dislocated shoulder* the arm is out of the joint, which can result from collisions in several sports.
3. *Rotator cuff injuries* involve a strain or tear in the four muscles around the shoulder (supraspinatus, infraspinatus, subscapularis, and teres minor) that hold the humeral head into the scapula. They are not uncommon in activities requiring the arm to be moved over the head many times (leading to the overuse of the shoulder), as in baseball pitching, swimming, weightlifting, andracket sports such as tennis.

Elbow

1. *Forehand tennis elbow (golfer's elbow, baseball elbow, suitcase elbow)* (*medial epicondylitis*) is due to forceful wrist flexion and pronation that can damage the tendons that attach to the medial epicondyle, and is common in tennis (when serving with topspin), pitching in baseball, and throwing a javelin.
2. *Backhand tennis elbow* (*lateral epicondylitis*) is caused when using the grasping and supination muscles. Damage occurs to the extensor tendons when the wrist is extended and to these muscles, such as during backhand returns in tennis.
3. A torn ulnar collateral ligament is common for baseball pitchers due to the overuse of the elbow. It is corrected by *Tommy John surgery*, as pioneered by Dr. Frank Jobe, in which the torn ligament is replaced by a tendon from somewhere in the body.

Hip

1. In a *hip flexor* there is damage to muscles around the hip.
2. In a *hip pointer* there is a bruise or fracture to the hip iliac crest (Figs. 2.14 and 2.15) and occurs in collisions in football and hockey.
3. *Avascular necrosis* is an injury due to collisions that results in a lack of blood supply to joint regions and their subsequent death. It is most common in the hips, but also is seen after collisions of the knees, shoulders, and ankles.

Legs

1. *Hamstring pulls*—as in: I pulled my "hammie"—are common in sports with much running, such as in track running and baseball, and occur in simultaneous (eccentric) contractions of the quadriceps and hamstrings, when the hamstrings are $<60\%$ as strong as the quadriceps muscles.
2. *Shin splints* are muscle pulls, often found in running.

Knee

1. Increasingly common are sprains or tears to the *anterior cruciate ligament (ACL)* (Fig. 1.3). Injuries to the ACL are not uncommon in skiing, basketball, soccer, and football when the leg is contorted at the knee and this ligament is excessively elongated.
2. *Runner's knee* is pain behind and on either side of the kneecap (patella), due to the rubbing of the kneecap against the lateral condyle of the femur (cartilage), and can result from downhill running and walking downstairs. Soreness in the tendons above and below the knee, *patella tendinitis,* can occur from repetitive overloading due to jumping and running.

Foot

1. *Turf toe* is a bruise to the last joint in the toe, the metatarsal phalangeal joint. It can occur from jamming the toe into turf, as in football collisions.
2. *Metatarsal stress fractures* (in the toes) are common in running due to pushing off from the toes.
3. *Plantar fasciitis* is an injury to the plantar fascia under the arch of the foot, and is seen in long distance running, squash, tennis, and basketball. (The fascia are the surrounding soft tissues.)
4. Injuries to the *Achilles tendon* (Figs. 1.8 and 3.34), including tendinitis (inflammation) or tearing is common in many sports with repetitive overloading, as in speed running, squash, and tennis, due to excessive tendon elongation. We have seen that the stresses in this tendon during running are not that far below the UTS.

Spine and Back

1. In a *herniated disc* a vertebral disc (Fig. 2.37) is displaced and presses against nerves. *Lower back pain* can also result when muscles in the lower back become strained or when the ligaments interconnecting the lowermost five vertebral bones become sprained *(lumbar strain)*. Such injuries can result during weightlifting, moderate lifting using back muscles instead of leg muscles, and sitting or lying down in positions that do not permit your spine to assume its natural curvature.

Generally to Bones and Cartilage

1. *Stress fractures* of bones are slight fractures due to repeated stress, such as to the foot or shins after excessive running.
2. *In a compound fracture* the bone breaks through the skin, and this can occur from collisions in skiing and football.
3. *Fractured ribs* can result from collisions. (Strains or tearing of intercostal muscles between the ribs can result from awkward motions such as overreaching.)

Injuries during games and practices in 15 common college sports occur most commonly in the legs ($\sim$54% of them), arms ($\sim$18%), trunk and back ($\sim$13%), and head and neck ($\sim$10%), and the injury rate per 1000 athlete exposures is $\sim$0.15 for anterior cruciate ligament injuries, $\sim$0.35 for concussions, and $\sim$0.8 for ankle ligament sprains (and, of course, each frequency is different for each sport) [33]. (An athlete exposure is defined as one athlete participating in one game or practice, in which he/she is exposed to the possibility of athletic injury.) For games, for men, the highest injury rate occurs for football (which is not surprising at all) ($\sim$36 per 1000 athlete exposures) followed by wrestling ($\sim$26), with baseball having the lowest injury rate ($\sim$6), and for women, the highest rate occcurs for soccer ($\sim$16) and the lowest occurs for softball ($\sim$4).

4.9 Avoiding Fractures and Other Injuries: Materials for Helmets

In this chapter we have discussed some of the consequences of collisions, i.e., bone breakage (and there are others, such as hematomas, etc.), and in Chap. 3 we briefly discussed how to lessen the effects of collisions by increasing the collision time and contact area. Helmets mitigate the effects of collisions of the head [55]. They consist of an outer shell and an interior liner. The shell transmits the impact load over the larger area of the liner, which absorbs most of the kinetic energy of the head. The hard shell of helmets also helps to prevent skull breakage. The cushioning material material and design appear to help decrease linear accelerations and the concussions they can cause, but apparently do not help decrease rotational acceleration and its effect. Helmets are now routinely used to lessen the effects of collisions and are used in football, hockey, skiing, cycling, and in some cases in baseball (by batters, with future use by pitchers possible). Soft headgear helmets are used by amateur boxers and by professional boxers during training. Face protection is common in ice hockey and football.

For a helmet to meet its goals for most of these activities, the shell must be rigid (i.e., be very stiff to resist deformation), tough (i.e., have high bulk strength to limit fracture), and hard (i.e., have high surface strength to prevent penetrating injuries), so that a large area of impact of the head into the liner can be maintained, and it should be light. The shell is often made from fiber-reinforced plastics (fiberglass/resin composites) and thermoplastics (such as polycarbonate).

Liners must be capable of being compressed and absorbing energy at a force level low enough so the peak force and acceleration felt by the head are minimized and the collision time is maximized. It is very good for the helmet cushion material to have high hysteresis. Figure 4.71 shows three types of materials, with very different force/deformation (stress/strain) curves. Type A is a linear spring and type C is a more realistic material. Type B is an ideal helmet material because it deforms at a constant stress, which is low enough to be of value in collisions. Figure 4.72 shows three materials. The shaded area, which is the work done on the material, is the same under each curve. For the stiff (large Y) and compliant (small Y) materials, the peak

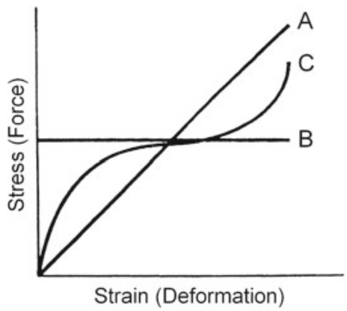

Fig. 4.71 Stress–strain curves for padding materials that could potentially be used in safety helmets. (From [55])

Fig. 4.72 Effect of the padding strength for the same energy absorbed. The peak force exceeds the maximum allowable force for the "strong" (or stiff) and "weak" (or compliant) materials. The weak material is crushed to just about its initial thickness and then becomes very stiff. (From [55])

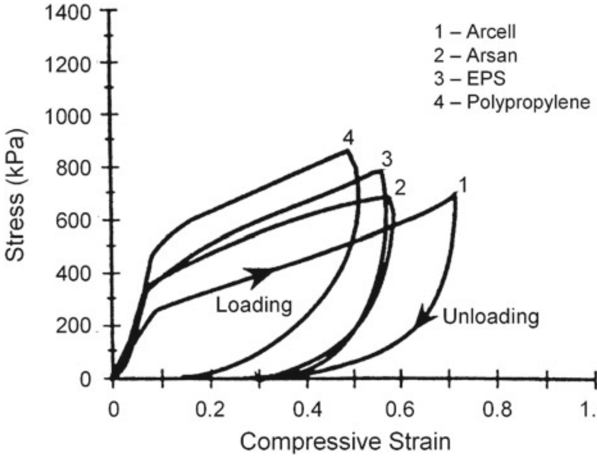

Fig. 4.73 Stress–strain for real padding materials: 1-Arcell, 2-Arsan, 3-EPS (expanded polystyrene), 4-Polypropylene. The energy absorbed is the area under the loading curve minus that under the unloading curve. (From [55])

force is very high at the end of deformation, while for the intermediate material, it is much smaller. This makes it a better material for a liner. (Ideally, the force should be independent of deformation, as for material B in Fig. 4.71.) The stress should be relatively independent of the strain rate, so the liner would work well at high and low impact speeds. As shown in Fig. 4.73, the material should deform plastically and have a large stress–strain hysteresis loop. Then the liner material absorbs the energy of the head impact and does not transfer it back to the head (during the collision),

Fig. 4.74 Helmeted impact deceleration with initial speed of 5.63 m/s. (From [55])

as would a compliant, spring-like material. If the helmet is to be used over and over again, the deformation or strain remaining after a cycle should be minimal. The area of impact of the head on the padding should be maximized. The thickness of the padding should be increased as much as possible, subject to weight and bulkiness constraints, because of limitations on how much it can be compressed during the impact. Also, when the padding is fully crushed, it becomes very stiff, resulting in high forces. (The maximum designed compression is about 80%.) Energy absorbing liners are usually made of semirigid polyurethane foams or expanded polystyrene bead foams. (Spongy bone at the end of long bones should have similar properties.) The deceleration while wearing a good helmet is shown in Fig. 4.74.

Decreasing the highest end of accelerations is most effective in decreasing the frequency of concussions. This can be done (and has been done) by improving helmet design, such as by using better materials and design, and includes the use of sectioned padding regions with air gaps so they can expand laterally when compressed, better padding contact with the mandible, and so on [13, 68]). Also, this can be done in sports by regulating the types of collisions that are allowed, such as by forbidding head contact during football tackling. There is still much to be learned about optimizing helmet design to minimize the rate of concussions during athletics [14].

4.10 Mechanical Properties of Food

While we do not want other objects to break our bones, we want our bones (really our teeth) to "break" or fracture food when we chew it, and so the desirable mechanical properties of food need to differ from those of the structural components of our bodies. Our ability to digest food efficiently (Chap. 6) depends on our ability to chew foods properly (Chap. 3) and the mechanical properties of the food [41, 43]. Our teeth are not designed to cut through the tough fibers in raw meat, even with extended chewing. It becomes easier to chew if the meat is first cooked and cut into small pieces. Making plants more useful foods involves breaking down cell walls and other fibers that are difficult to digest. During chewing, at low stress foods elastically deform, and with successively increasing stress they plastically deform, then crack, and then these cracks propagate across them.

Stiff foods, such as apples and crackers, have large Young's moduli (called E in this community instead of Y) and so high stresses (and forces) are required to crack them. These hard foods have large values of $(ER)^{0.5}$, where R is the toughness (area under the force-area curve divided by the crack area, which is related to the energy needed to break bonds during cracking, and which is also called W_{F}). They have a concave-down stress-strain curve as in Fig. 4.18, sometimes called r-shaped, and are called force-limited or $(ER)^{0.5}$ foods. The incisors create high stress and are used to crack these foods without the need of the tooth cusp to continue the crack development or displacement. The crunchiness you hear when eating some foods, such as raw carrots, is due to mini sonic booms in your mouth when the crack propagation speeds exceeds the speed of sound, because the energy being released during crack propagation is much larger than the toughness [65, 67, 76].

More compliant foods, such as meat or spinach, are not stiff and require much energy to tear them or slice them apart, and consequently they have high toughness, due to collagen (in meat) or cellulose (in plants). Such tough foods have high $(R/E)^{0.5}$ and have a concave up stress-strain curve as in Fig. 4.21, sometimes called J-shaped, and are called displacement-limited or $(R/E)^{0.5}$ foods; for these foods the tooth cusp needs to continue the crack displacement once fracture starts. Lateral and forward/backward motions of the molars are used to break down these foods. Figure 4.75 illustrates the increase in number of food particles with continued chewing.

The forms for these scaling parameters are not surprising given the discussions earlier this chapter. The threshold for a crack to propagate, K, varies as $(GY)^{0.5}$ at threshold according to (4.97), which is $(ER)^{0.5}$ with $E = Y$ and $R = G$ as is common in this field, so it is reasonable that this is the scaling parameter when force is the limiting factor. Crack propagation is expected using the three-point configuration for bone bending in Fig. 4.26, where the F_1 and F_2 points of contact can now be two cusps on a molar in the lower jaw, with F applied from a cusp from a tooth in the upper jaw. The threshold stress for fracture and propagation varies as E according to (4.81), so in this case $(ER)^{0.5}$ divided by E, or $(R/E)^{0.5}$, could be a good scaling parameter [43].

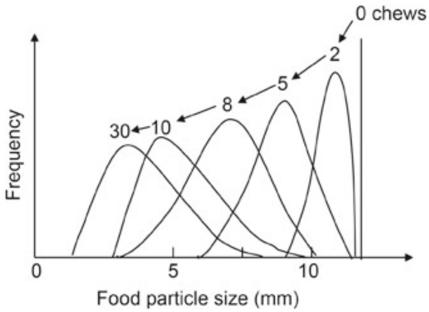

Fig. 4.75 Schematic of the particle size distribution when chewing a piece of a raw carrot, illustrating the increasing number of pieces (comminution) with the number of chews. (Based on [43])

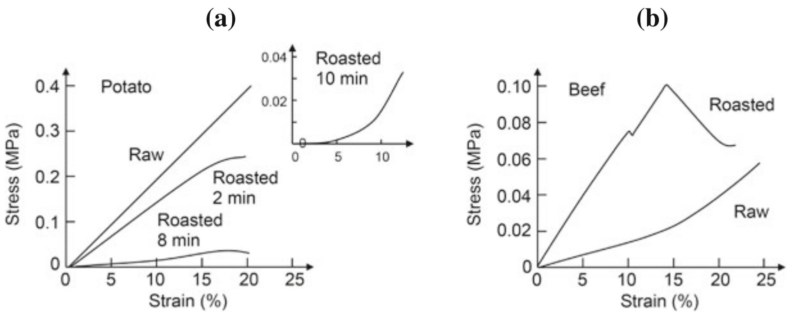

Fig. 4.76 Effect of cooking on the mechanical properties of **a** a potato by boiling (including inset) and **b** beef by roasting. (Based on [41, 43])

Processing and cooking food serve several functions [41, 43]. For example, cooking makes nutrients more accessible, inactivates toxins in foods, extends food storage time, and makes food easier to chew. Cooking denatures collagen, bursts cells, and softens cellulose and this helps us fracture foods when we chew them. As seen in Fig. 4.76a, boiling decreases the Young's modulus and toughness of potatoes (they are more tender and less stiff), making them easier to fracture during biting. The toughness of a potato decreases from 225 J/m^2 when raw to 38 J/m^2 after 10 min of boiling and the stress-strain curve becomes J-shaped [43]. Roasting decreases the toughness of the flesh inside of a potato to 59 J/m^2 and the casing to 123 J/m^2. Raw meat is so compliant and tough because it has much collagen, and it is difficult to fracture. As seen in Fig. 4.76b, roasting beef increases its Young's modulus, which allows fractures to propagate easier and makes it more chewable. Processing and cooking food makes it easier to fracture, so less force is needed during chewing, fewer chews are needed, and the utilization of the nutrients in food is improved, so we need to eat less food. Figure 4.77 shows that the stress-strain relation of foods, in this case Gouda cheese, also depends on age and on strain rate [76].

Fig. 4.77 The stress-strain curve of Gouda cheese depends on age (straight lines for two weeks old, dashed line for one year old), and on strain rate. (Based on [76])

4.11 Summary

Understanding the stress, strain, and fracture of body materials and parts is essential to explain the performance of the human machine under normal and extraordinary conditions. Time-independent material models, describing harmonic and non-harmonic elastic behavior, and time-dependent viscoelastic models can be used to characterize and understand the stress–strain relations of the body materials and components. The mechanical properties of the many parts of the body involved in structure, motion, and organ operation, are all very different; these properties depend on their composition, structure, and composite nature. The deformation of extended body parts, such as the bending of bones, and the mechanics of fracture are needed to analyze the body under extreme conditions that can lead to injury.

Problems

Stress and Strain

4.1 Determine the spring constant, k, in SI units for a solid cylinder of cortical bone of length 0.5 m, diameter 2 cm, and $Y = 17.4\,\text{GPa}$.

4.2 A cylindrical spring of length 2 cm and diameter 3 mm has spring constant $k = 1.7 \times 10^5\,\text{N/m}$.
(a) How much does it extend when a force of 100 N is applied to it?
(b) What is the strain?
(c) The spring is composed of a uniform material. Find its Young's modulus (in MPa).

4.3 Equation (4.8) shows how Young's modulus, the shear modulus, and Poisson's ratio are interrelated for an elastic isotropic material. The bulk modulus B is the negative of the pressure divided by the fractional change in volume caused by that pressure, and it can be related to any two of these three above parameters. Show that